Published in final edited form as:
Neuroscience. 2007 November 23; 149(4): 943–961. doi:10.1016/j.neuroscience.2007.07.067.

A CHRONIC HISTOPATHOLOGICAL AND ELECTROPHYSIOLOGICAL ANALYSIS OF A RODENT HYPOXIC-ISCHEMIC BRAIN INJURY MODEL AND ITS USE AS A MODEL OF EPILEPSY

Philip A. Williams[1] and **F. Edward Dudek**[2]
Dept. of Biomedical Sciences, Neurobiology Section, Colorado State University, Fort Collins, CO 80523 USA

Abstract

Ischemic brain injury is one of the leading causes of epilepsy in the elderly, and there are currently no adult rodent models of global ischemia, unilateral hemispheric ischemia, or focal ischemia that report the occurrence of spontaneous motor seizures following ischemic brain injury. The rodent hypoxic-ischemic (H-I) model of brain injury in adult rats is a model of unilateral hemispheric ischemic injury. Recent studies have shown that an H-I injury in perinatal rats causes hippocampal mossy fiber sprouting and epilepsy. These experiments aimed to test the hypothesis that a unilateral H-I injury leading to severe neuronal loss in young-adult rats also causes mossy fiber sprouting and spontaneous motor seizures many months after the injury, and that the mossy fiber sprouting induced by the H-I injury forms new functional recurrent excitatory synapses. The right common carotid artery of 30-day old rats was permanently ligated, and the rats were placed into a chamber with 8% oxygen for 30 min. A quantitative stereologic analysis revealed that the ipsilateral hippocampus had significant hilar and CA1 neuronal loss compared to the contralateral and sham-control hippocampi. The septal region from the ipsilateral and contralateral hippocampus had small but significantly increased amounts of Timm staining in the inner molecular layer compared to the sham-control hippocampi. Three of 20 lesioned animals (15%) were observed to have at least one spontaneous motor seizure 6–12 months after treatment. Approximately 50% of the ipsilateral and contralateral hippocampal slices displayed abnormal electrophysiological responses in the dentate gyrus, manifest as all-or-none bursts to hilar stimulation. This study suggests that H-I injury is associated with synaptic reorganization in the lesioned region of the hippocampus, and that new recurrent excitatory circuits can predispose the hippocampus to abnormal electrophysiological activity and spontaneous motor seizures.

Keywords

Epilepsy; sprouting; recurrent excitation; population spikes; epileptiform bursts

Correspondence to: F. Edward Dudek, Ph.D. Department of Physiology, University of Utah School of Medicine, 420 Chipeta Way, Suite 1700, Salt Lake City, UT 84108, (801) 587-5880, ed.dudek@hsc.utah.edu.
[1]Current address: Department of Neurosciences, Case Western Reserve University School of Medicine, Cleveland, OH;
[2]Current address: Department of Physiology, University of Utah School of Medicine, Salt Lake City, UT.

One common chronic complication following ischemic brain injury is the later development of chronic spontaneous recurrent seizures (Pohlmann-Eden et al., 1996; Olsen, 2001). Factors associated with ischemic brain injury and epilepsy are poorly defined, but it appears that large cortical lesions have a strong association with the later appearance of seizures (Berges et al., 2000; Lamy et al., 2003). Currently, the occurrence of chronic spontaneous recurrent motor seizures have been observed in only one rodent model of focal ischemia (cortical photothrombosis, Karhunen et al. 2007), but not in focal ischemia induced by middle cerebral artery occlusion (Karhunen et al. 2003, 2006) nor in global ischemia (Epsztein et al., 2006).

Global forebrain ischemia following cardiopulmonary arrest in humans has been shown to cause delayed hippocampal neuronal loss (Petito et al., 1987). The rodent model commonly used to analyze this type of brain injury is the four-vessel occlusion model (Pulsinelli and Brierley, 1979, Pulsinelli et al., 1982). An earlier alternate to this model was implemented by Levine (1960), and modified by Rice et al. (1981); it used a combination of hypoxia and ischemia to cause brain injury (relative oligemia rather than a true ischemia; see Ginsberg and Busto, 1989 for review). This hypoxia-ischemia (H-I) model is commonly used in postnatal-day-7 (P7) rats to induce a brain injury similar to neonatal H-I in humans. Unilateral H-I lesions in P7 rats have recently been shown to cause mossy fiber sprouting in the inner molecular layer (IML) of the dentate gyrus in both the lesioned and unlesioned hippocampi (Williams et al., 2004). Chronic spontaneous motor seizures were observed months after the H-I lesion in approximately 40% of the injured rats (Williams et al. 2004). Towfighi et al. (1997) reported that neuronal susceptibility to an H-I injury shifts as a function of age. The most susceptible hippocampal neurons in H-I injured P7 rats are thought to be the CA3 pyramidal neurons, followed by the CA1 pyramidal neurons, and then the dentate gyrus and the hilus (Towfighi and Mauger, 1998). In contrast, 30-day old rats subjected to an H-I insult showed that CA1 and the hilus appeared to be the more susceptible neuronal populations, with relative sparing of CA3 and the dentate gyrus. The pattern of neuronal loss in 30-day H-I rats is similar to what is seen in adult rats that undergo global forebrain ischemia by the four-vessel occlusion method and in humans after global forebrain ischemia following cardiopulmonary arrest (Pulsinelli and Brierley, 1979, Pulsinelli et al., 1982, Petito et al., 1987). The pattern of injury in the hippocampus after a hypoxic and/or ischemic insult has many general similarities to the histopathological abnormalities associated with temporal lobe epilepsy; one of the central features of human temporal lobe epilepsy is Ammon's Horn Sclerosis, where neurons in the hilus and in the CA3 and/or CA1 areas are lost (Babb and Brown, 1987; Franck and Roberts, 1990).

In human temporal lobe epilepsy (Houser et al., 1990), and in both the kainate and pilocarpine models of status epilepticus with subsequent epileptogenesis in rats (Nadler et al., 1980; Mello et al., 1993), Timm staining and other anatomical techniques have shown that the mossy fibers of the dentate granule cells innervate the inner molecular layer (IML) of the dentate gyrus, a condition that is not usually present in normal animals or humans (Buckmaster and Dudek, 1997a, b, 1999). Onodera and coworkers (1990) showed that the four-vessel occlusion model of global forebrain ischemia is associated with abnormal Timm staining in the IML, although the amount of Timm staining in the IML was substantially less than in the kainate- or pilocarpine-models of temporal lobe epilepsy. The presence of mossy fiber sprouting in the hippocampus may act as a marker of the formation of new recurrent synapses in other areas of the brain and of the potential for the development of epilepsy (Gorter et al., 2001).

The hypothesis that Timm stain in the IML and associated mossy fiber sprouting leads to enhanced recurrent excitation, and could contribute to epileptogenesis in the dentate gyrus, was advanced by the experiments of Tauck and Nadler (1985). They showed that mossy fiber sprouting in kainate-treated rats was associated with paired-pulse potentiation and multiple population spikes to hilar stimulation, which would be expected to activate primarily the mossy

fiber axons of the dentate granule cells. Subsequent experiments revealed that in most preparations from kainate-treated rats, the responses to hilar and perforant path stimulation were relatively normal or only slightly abnormal in standard media (Cronin et al., 1992; Patrylo and Dudek, 1998); however, when $GABA_A$-mediated inhibition was blocked with bicuculline, some preparations with mossy fiber sprouting showed bursts to hilar stimulation, while those without sprouting did not show bursts. Some of these bursts had a long and variable latency when evoked at low stimulus intensities, a characteristic expected of circuits with recurrent excitation (Traub and Wong, 1982; Miles and Wong, 1986, 1987; Christian and Dudek, 1988a, b). If synaptic reorganization occurs after H-I and is similar to the kainate model, then local inhibitory circuits may mask recurrent excitation, and one method used to reveal these new excitatory synapses is to block or depress inhibition and/or raise the concentration of extracellular potassium (Traub and Wong, 1982; Miles and Wong, 1986, 1987; Christian and Dudek, 1988a, b; Cronin et al., 1992; Wuarin and Dudek, 1996, 2001; Patrylo and Dudek, 1998; Hardison et al., 2000; Lynch and Sutula, 2000;). Another method used to demonstrate the formation of new recurrent excitatory synapses is focal flash-photolysis of caged-glutamate, which has been used to map neuronal circuitry and the formation of these new circuits (Callaway and Katz, 1993; Katz and Dalva, 1994; Dalva and Katz, 1994; Wuarin and Dudek, 1996, 2001; Molnar and Nadler, 1999).

Studies that have examined neuronal and network excitability after global forebrain ischemia have had varied results. Mody and coworkers (1995) reported that inhibition was intact in granule cells 3 months after 15 min of global ischemia, and that hyperexcitability was not present. Furthermore, a decrease in the excitability of CA1/CA2 pyramidal neurons was observed in rats 10–12 months after global ischemia (Arabadzisz et al., 2002). Hyperexcitability, a reduced threshold for burst generation, and interictal epileptiform discharges have been reported in the CA3 region chronically after global ischemia (Congar et al., 2000; Wu et al., 2005; Epsztein et al., 2006). However, chronic spontaneous seizures after global forebrain ischemia have not been reported in the literature.

The goal of this study was to use an H-I model in 30-day-old rats to create a large unilateral lesion in the cortex and hippocampus. This would in turn allow an evaluation and comparison of the potential for mossy fiber sprouting in the IML and chronic spontaneous motor seizures in this model (i.e., 30-day hypoxia-ischemia) with the perinatal model of hypoxia-ischemia and with the four-vessel occlusion model of global forebrain ischemia. This study tested the hypothesis that the neuronal loss caused by an H-I injury at 30 days of age would be associated with synaptic reorganization in the hippocampus, and that these new circuits would lead to abnormal electrophysiological responses in the dentate gyrus. We performed a septo-temporal analysis of Timm staining in the IML and a quantitative stereologic assessment of the hippocampus to address the first part of this hypothesis. The second part of the hypothesis was examined with *in vitro* extracellular and whole-cell patch-clamp recordings with focal flash photolysis of caged glutamate in hippocampal slices from H-I injured rats and age-matched controls many months after the H-I lesion. We further hypothesized that these rats following an H-I injury at 30 days of age would develop chronic spontaneous motor seizures, and that this model of unilateral hemispheric brain injury may have use as a model of epilepsy.

EXPERIMENTAL PROCEDURES

Surgical preparation

A modified version of the Levine preparation, as described by Rice and coworkers (1981), was used to create an H-I injury in the right hemisphere. Sprague-Dawley rats (both male and female, 30 days of age, n=29 H-I treated animals and 13 sham-surgical controls) were anesthetized using a 2% isoflurane/oxygen mixture. The ventral midline of the neck was surgically prepared and infused with bupivicaine (0.5%, 0.5 ml). A 1-cm ventral-midline

incision was made, and the right common carotid artery exposed and permanently double ligated with 4-0 dexon. The skin was closed with 4-0 dermalon, and the rats were allowed to recover in a heated cage. For the sham controls, the carotid artery was exposed but not ligated. After 2 h of recovery, the H-I treated rats were placed in an airtight chamber where the temperature and humidity were maintained at 37° C and 90%, respectively. The chamber was then filled with an 8% oxygen and 92% nitrogen mixture. The oxygen content of the chamber was monitored with an oxygen-sensitive electrode (Microelectrode, Inc). The rats were exposed to 8% oxygen for 30 min and then allowed to recover in room air.

Behavioral monitoring of motor seizures

After surgery, all rats were observed for occurrence of chronic motor seizures. All rats prior to the histological and electrophysiological experiments were directly monitored for an average of 6 h per week for a duration ranging from 6 to18 months by a trained observer who was blind to the animals' treatment. Control animals were observed alongside the treated rats for the duration of the study. Only grade 3 seizures or higher (Racine, 1972) were recorded. Grade 3 seizures were characterized by forelimb clonus, with grade 4 seizures showing forelimb clonus and rearing, and grade 5 seizures resembling grade 4 seizures with the addition of the loss of the righting reflex.

Slice preparation and in vitro electrophysiological studies

For electrophysiological experiments in hippocampal slices, rats were anesthetized (sodium pentobarbital, 100 mg/kg, IP) and euthanized by decapitation. The brain was rapidly removed and stored for 1 min in ice-cold physiological solution (composition in mM: 124 NaCl, 3 KCl, 1.3 $CaCl_2$, 26 $NaHCO_3$, 1.3 $MgSO_4$, 1.25 NaH_2PO_4, 10 glucose equilibrated with 95% O_2, 5% CO_2, pH 7.2–7.4). The brain was bisected along the mid-line, with either the ipsilateral or the contralateral hemisphere randomly selected for a particular electrophysiological experiment. The occipital pole was blocked and glued to the vibroslicer chuck in order to cut 300–400 μm-thick coronal slices of the septal (i.e., dorsal) hippocampus in a rostral-to-caudal direction (i.e., cut from the frontal cortex toward the occipital pole). The slices were kept in a storage chamber and allowed to equilibrate for 1.5–2.0 h prior to initiation of the recordings, and their precise order was maintained so that their location along the septo-temporal axis of the hippocampus was known. The opposite hippocampus was used for anatomical studies. Slices were studied electrophysiologically in recording chambers that allowed multiple stimulating and recording electrodes.

Histology

A modified Timm histological procedure was used to label the zinc-containing axons of the granule cells. The hippocampus that was not used for *in vitro* electrophysiological experiments was dissected from the hemisphere and prefixed in phosphate buffered Na_2S (0.37%) to precipitate the zinc in the mossy fibers. The hippocampus was emersion fixed in phosphate buffered 4% paraformaldehyde (pH=7.2). The tissue was then saturated with 30% sucrose and sectioned at 35 μm on a sliding microtome. The hippocampus was straightened prior to mounting on the microtome (Buckmaster and Dudek, 1997b). Every sixth section was mounted for Timm staining with cresyl-violet counter-stain, and the adjacent sections were mounted for cresyl-violet staining alone. The first section selected for the start of the series was randomly selected using a random number generator. Following the electrophysiological experiments, the recorded slices were fixed and processed for Timm staining in the same fashion as described for the entire hippocampus, except that every section from the recorded slices was mounted and processed for Timm-stain analysis. All of the sections were coded and the intensity of the Timm stain in the IML was graded with blind procedures according to a modified rating scale of Tauck and Nadler (1985). In this subjective rating system, a lack of Timm staining in the

IML was scored a 0; small amounts of sparsely scattered Timm stain throughout the IML was scored a 1; dark areas of Timm staining that formed a discontinuous band of Timm staining in the IML was scored a 2; and a continuous dark band of Timm staining in the IML extending along the inner to the outer blades of the dentate gyrus was scored a 3 (no scores of 3 were seen in this study). This scale was modified to allow "0.5" scores (i.e., half scores), such that when two scores from individual sections were averaged together, the mean could be rounded to the nearest half score to increase the resolution of the scoring system (i.e., two sections from the same hippocampus with scores of 0 and 1 would average to 0.5). The sections were grouped according to their location along the septo-temporal axis (i.e., 25% was defined as the septal end, and 100% was defined as the temporal end). The Timm-stain grades for each section in a group were summed and then divided by the total number of sections/group to determine a mean Timm score for each region. The Timm score for each region was then averaged and a median score was found for each treatment. The treatments were then compared using analysis of variance (ANOVA) with a non-parametric Kruskal-Wallis test.

Stereology

Neuronal counts of the hilus and CA1 were estimated using the optical fractionator probe (West et al., 1991) in the counting software Stereoinvestigator (MicroBrightField; Colchester, VT). The cresyl-violet-stained sections were used to estimate the total number of neurons, and the sections were coded so that the investigators performing the counts were blind to the treatment. Neurons were defined by their large nuclei with hypochromatic vesiculated chromatin and prominent nucleoli. Only those nuclei that came into focus while focusing down through the dissector height were counted. The counting frame for the hilus was 65 μm × 65 μm with a counting grid of 150 μm × 150 μm and an average of 17 sections per hippocampus, the counting frame for CA1 was 30 μm × 30 μm with a counting grid of 120 μm × 120 μm and the same number of hippocampal sections. The counting frame was randomly placed throughout a defined area of the hilus and CA1 region. The hilus was defined as the region from the apex of CA3 extending as diagonal lines to the inner tips of both the inner and outer blades of the granule cell layer and extending around the inner margin of the granule cell layer up to the apex of the dentate gyrus. The CA1 region was defined by the region of densely packed small pyramidal neurons adjacent to the more loosely packed larger neurons comprising CA2 up to the region where neurons began to form the tri-laminar subiculum region. The average counting coefficient of error (West et al., 1991) for control hippocampi was 0.06 for both the hilus and CA1. The estimated counts for each section were grouped along the septal-temporal axis as described for the Timm-stain analysis. Each region contained no less than three sections. Neuronal counts for each region were then derived using the formula from West and coworkers (1991). The estimated counts from each region were then averaged for each treatment group. Each region for the treatment groups was compared to each other using an ANOVA with a student-Newman-Keuls test (SNK).

Extracellular Recordings

Extracellular electrodes were filled with 1 M NaCl (2–20 MΩ). Bipolar stimulating electrodes were made of two tightly wound Teflon-coated platinum-iridium wires (75 μm diameter, SIU-SC100, Winston Electronics, Millbrae, CA; Grass S88, Quincy, MA). The recording pipette was placed into the granule cell layer, and the bipolar stimulating electrode was placed in the hilus to evoke population spikes via antidromic stimulation of the mossy fibers. Recordings were initially obtained in control solution (ACSF). Five antidromic stimulus intensities, based upon the minimum current needed to evoke a 0.5 mV amplitude population spike (minimum, 2X-minimum, 4X-minimum, 8X-minimum, and 16X-minimum), were used to assess and normalize population spike responses. Five responses were evoked and averaged for each of the different stimulus intensities at a rate of 0.05 Hz, and responses were averaged prior to analysis. Slices that could not produce a population spike amplitude to antidromic hilar

stimulation of 5 mV or greater were not included in the analysis. The hippocampal slices were then bathed in 30 μM bicuculline and the stimulation protocol was repeated, as was established in the control solution. While still in 30 μM bicuculline, the extracellular potassium was raised from 3 mM to 6 mM, and the stimulation protocol was again repeated. The glutamate receptor antagonists DL-2-amino-5-phosphonovaleric acid (AP-5, Sigma, 50 μM) and 6, 7-dinitroquinoxaline-2, 3, (1H, 4H)-dione (DNQX, Sigma, 50 μM) were used to assess the role of glutamatergic synapses in the generation of population spike bursts. After the completion of the recordings, the slices were individually fixed for Timm-stain analysis.

Whole-cell patch-clamp recordings

For the whole-cell recordings, two to four 300 μm-thick slices were kept for 1–2 h in oxygenated ACSF at 32° C before being transferred to the recording chamber where recordings were obtained at room temperature (21–23° C). Perfusion solution (10 ml) containing caged glutamate (L-glutamic acid, γ-(α-carboxy-2-nitrobenzyl) ester (250 μM), Molecular Probes, Eugene, OR) was oxygenated and recirculated at 2 ml/min. Pipettes for whole-cell recordings were made from borosilicate glass capillaries (KG-33, Garner Glass, Claremont, CA) with a horizontal pipette puller (P-87 Flaming-Brown pipette puller, Sutter Instruments, Novato, CA) to an open resistance of 2–4 MΩ. Pipette solution contained (in mM) 140 K-gluconate, 10 N-2-hydroxyethylpiperazine-N′-2-ethanesulfonic acid (HEPES), 1 NaCl, 1 $CaCl_2$, 1 $MgCl_2$, 5 ethylene glycol-bis (β-aminoethyl ether)-N, N, N′, N′-tetraacetic acid (EGTA), and 4 magnesium ATP, pH 7.2. The data were not used if the resting membrane potential was less than −70 mV when whole whole-cell configuration was obtained. Whole-cell currents were amplified with an Axopatch-1D amplifier (Axon Instruments, Foster City, CA), filtered (2 kHz), digitized (44 kHz) and stored on video tapes (Neuro-Corder, Neurodata Instruments, New York, NY). Data analysis was done off line with sampling rates of 5–10 kHz (pClamp 6, Axon Instruments). Recording and analysis of the electrophysiological data was done without knowledge of the treatment. The Fisher's exact test was used to test for differences in the effects of the flash photolysis of caged glutamate between the different treatment groups.

Flash-photolysis of caged-glutamate

Uncaging of glutamate (Callaway and Katz, 1993) was obtained with a xenon flash lamp (Chadwick-Helmuth, El Monte, CA). The flash of ultraviolet light was transmitted through a high-numerical-aperture, oil-immersion objective (X40, Nikon) mounted underneath the bottom of the recording chamber (coverslip) and focused approximately 200 μm into the tissue. A HeNe laser aimed directly through the objective into the tissue was used to determine the location of the photostimulation. A monochrome CCD camera (Cohu, San Diego, CA) and video monitor were used to determine the location of, and the distance between, the recorded cells and the laser-light locator. Flashes with intensities 50–100 mJ, combined with a bath concentration of caged glutamate of 250 μM, produced a spatial resolution of approximately 100 μm. Consequently, photostimulations were applied in the granule cell layer at sites 150 μm apart.

RESULTS

Neuron Loss

Of the 29 treated rats, 20 had gross lesions consisting of severe loss of neuronal tissue in the ipsilateral frontoparietal cortex (i.e., cortical thinning) and the septal-to-middle hippocampus (i.e., severe hippocampal sclerosis) that were noted at the time of euthanasia, and no gross lesions were seen in the contralateral or control hippocampi. Histologic analyses were performed on 8 ipsilateral hippocampi from lesioned rats, 12 contralateral hippocampi from lesioned animals, and 13 hippocampi (right and/or left) from sham-control rats. In order to assess the extent of the H-I injury to the hippocampus, neuronal loss was quantified in the hilus

and CA1 region throughout the septo-temporal axis of the hippocampus using the optical fractionator method (West et al., 1991). A qualitative assessment based on visual examination of the hippocampus showed that the H-I lesion appeared to be limited to the septal half of the ipsilateral hippocampus. Specifically, the H-I lesion appeared to involve severe loss of CA1 and hilar neurons, while CA3 seemed relatively intact (Fig. 1). A quantitative assessment of hilar and CA1 neurons (CA3 was not quantified) revealed that hilar neuron loss in the ipsilateral hippocampus was significant throughout the extent of the septotemporal axis (Fig. 2A) when compared to the contralateral and sham control hippocampi, which did not have significantly different neuron counts in either the hilus or CA1. However, the temporal (100%) ipsilateral hilus was not significantly different from the contralateral temporal hilus, but it was significantly different from the sham controls at the temporal end. The CA1 region of the ipsilateral hippocampus demonstrated significant neuron loss (Fig. 2B) up to the temporal end where neuron counts of CA1 were not significantly different from either the contralateral or sham control hippocampi. The relative decrease in the number of neurons (i.e., neuron loss) was much greater in the septal area than the temporal area, for both CA1 and hilus. Hilar neuron loss was positively correlated with CA1 neuron loss (Fig. 2C), indicating that the severity of CA1 neuron loss closely matched hilar neuron loss. These data indicate that the H-I lesion, as it affects the hippocampus, was most severe in the septal hippocampus, but the injury did to a lesser extent involve the temporal end. These data also suggest that the contralateral hippocampus was not directly injured by unilateral ligation and global hypoxia.

Mossy fiber sprouting

Both hippocampi, ipsilateral and contralateral to the H-I injury, were examined for Timm stain in the IML to assess for the presence of mossy fiber sprouting. A small but significant amount of Timm stain was found in both the ipsilateral and contralateral septal hippocampi from the H-I injured rats, as compared to the sham control animals (Fig. 3 and 4). The temporal hippocampus did not show an increase in Timm stain in the IML for either the ipsilateral or contralateral hippocampi. This finding is similar to the results of Onodera and coworkers (1990) in the four-vessel occlusion model. Mossy fiber sprouting and hilar neuron loss showed a weak negative correlation throughout the entire hippocampus (r^2=−0.20, p=0.001; i.e., Timm stain scores increased with a decrease in hilar neurons) with specific correlations occurring in the middle region of the hippocampus (i.e., 50% and 75% septotemporal axis; r^2=−0.41, p=0.0002; r^2= −0.14, p=0.047 respectively, data not shown), but not in the septal and temporal ends (r^2=0.06 and r^2=0.02 respectively, data not shown), implying that the small amount of mossy fiber sprouting that was induced by H-I injury was weakly related to the amount of hilar neuronal loss that occurred.

Extracellular electrophysiology

Extracellular recordings were obtained in 27 ipsilateral hippocampal slices from 9 H-I lesioned animals and contralateral data in 21 hippocampal slices from 7 lesioned animals. From the 13 sham-control animals, 36 hippocampal slices were obtained and used for this analysis. The septal hippocampi from the control and H-I treated animals were assessed for abnormal electrophysiological responses several months after treatment. Hippocampal slices were studied by recording with extracellular electrodes placed into the granule cell layer, while a bipolar stimulating electrode was positioned in the hilus for antidromic stimulation of the mossy fibers. In normal ACSF, hilar stimulation produced a single antidromic population spike in slices from control animals (Fig. 5A) and in slices from experimental animals several months after H-I treatment (Fig. 5B). Similar responses were seen in hippocampal slices bathed in 30 μM bicuculline from both control and experimental animals (data not shown).

When slices from control animals were bathed in 6 mM $[K^+]_o$ and 30 μM bicuculline and stimulated in the hilus, the typical response of the granule cells was a single antidromic

population spike (Fig 5C), similar to the response in normal ACSF (Fig 5A). Some slices from control animals produced multiple population spikes in 6 mM $[K^+]_o$ and 30 μM bicuculline, but had a graded response as a function of stimulus intensity (i.e., the number of population spikes increased in a linear fashion as the stimulus intensity was increased (Fig. 6A)). A graded response was considered a control response, as has been demonstrated in previous studies (Patrylo and Dudek, 1998). A graded response is likely evoked by the recruitment of additional mossy fiber axons, hilar mossy cells, potential CA3 to mossy cell connections, and even the perforant path at very high stimulus intensities. The hilar-evoked responses from rats that had been treated with H-I several months before the in vitro electrophysiological experiments included all-or-none bursting, after-discharges of population spikes and synaptic responses with long and variable latency (Figs. 5D and 6B). An all-or-none burst was defined as a four-fold or greater increase in the number of population spikes at a low or near-minimal stimulus intensity (i.e., the lowest stimulus intensity that still evoked a detectable response). To fulfill the criteria for an all-or-none burst, a weak stimulus also had to result in at least one burst failure (Fig. 6B). A graded response was never seen to have a four-fold or greater increase in population spike numbers at a low or near-minimum stimulus intensity. It is important to make this distinction between the two types of population spike bursts to avoid confusion concerning an analysis of graded versus all-or-none bursts in our study with a less specific analysis – namely, the presence or absence of hippocampal "hyperexcitability." The hallmark of network activity from recurrent excitatory circuits is all-or-none network bursts with a long and variable latency to extracellular stimulation in an isolated region of a hippocampal slice, as has been demonstrated in both the normal CA3 (Traub and Wong, 1982;Miles and Wong, 1983;Miles and Wong, 1987) and the dentate gyrus of kainite-treated rats with mossy fiber sprouting (Cronin et al., 1992;Patrylo and Dudek, 1998,Wuarin and Dudek, 1996,2001). Hilar stimulation did not produce all-or-none bursts of population spikes in any of the slices from sham control or H-I animals in control solution, and all-or-none bursts of population spikes to hilar stimulation in 30 μM bicuculline and 6 mM $[K^+]_o$ were never seen in the sham control animals. Only single antidromic spikes or graded burst responses were elicited when control slices were bathed in 6 mM $[K^+]_o$ and 30 μM bicuculline (100% of the control animals; Figs. 5C and 6A). In 6 mM $[K^+]_o$ and 30 μM bicuculline, 52% of the slices from the ipsilateral hippocampi and 48% of slices from contralateral hippocampi of H-I treated rats generated responses that were abnormal (i.e., all-or-none bursts) compared to hippocampal slices from control animals in 6 mM $[K^+]_o$ and 30 μM bicuculline (single antidromic spike [Fig. 5C] or graded burst [Fig 6A]). The proportion of hippocampal slices with abnormal bursts from the ipsilateral and contralateral hippocampi was significantly different from the control animals ($p=0.007$ and $p=0.01$, Fisher's exact test). When only all-or-none bursts of population spikes were assessed as a subset of abnormal bursting in ipsilateral and contralateral hippocampi, 30% of the ipsilateral and 15% of the contralateral slices had all-or-none bursting, which were both significantly different from the control slices (0%, $p=0.0006$ and $p=0.04$ respectively, Fisher's exact test). In a small proportion (11%) of the ipsilateral slices, successive stimuli (0.05 Hz) at a constant stimulus intensity in 30 μM bicuculline and in 6 mM $[K^+]_o$ triggered bursts of population spikes that slowly increased in duration until prolonged bursts (i.e., 1–2 sec) were observed. The average and median Timm score for ipsilateral and contralateral slices showing all-or-none bursting was 1 with a range of 0.5–2.0, and the average and median Timm score for ipsilateral slices without all-or-none bursting was 0 with a range of 0–0.5 ($p<0.05$, Kruskal-Wallis). In all of the slices that demonstrated all-or-none bursting to hilar stimulation, application of 50 μM AP-5 and 50 μM DNQX blocked the bursts of population spikes, and the response recovered after several hours of wash out (Fig. 7). These data show a significantly increased probability of abnormal electrophysiologic responses in H-I injured hippocampi compared to slices from control animals under identical recording conditions, but the differences were only detected when the slices were compared in bicuculline and 6 mM $[K^+]_o$. These abnormal responses appeared to involve glutamatergic mechanisms, which suggest that new excitatory synapses had formed in the dentate gyrus.

Flash photolysis

Focal stimulation with application of glutamate microdrops and photoactivation of caged glutamate has been shown to evoke repetitive EPSPs and EPSCs in hippocampal slices from kainate-treated rats with Timm stain in the IML (Wuarin and Dudek, 1996, 2001; Molnar and Nadler, 1999). With flash photolysis of caged glutamate, we tested the hypothesis that H-I treatment leads to an increase in the number of granule cells showing repetitive EPSCs, when compared to slices from control animals. Photostimulations were first applied directly on the recorded granule cell to confirm that the flash of UV light uncaged glutamate and produced action potentials. The spot was then moved away from the recorded cells in 150 μm steps, first on one side of the recorded cell and then on the other side, until reaching the tip of the granule cell layer. Each location was stimulated several times (≥3 stimulations per location) and the presence or absence of repetitive EPSCs was assessed with whole-cell recordings at resting membrane potential. The response to photostimulation was consistent for a given location (i.e., photostimulation evoked repetitive EPSCs every time or it never evoked repetitive EPSCs). Thus, for each stimulation location, the response was positive every time or negative every time (Fig. 8). None of 16 granule cells tested in slices from sham-surgical control animals (0%, n=6 rats) showed repetitive EPSCs in response to photostimulation. In contrast, photostimulation evoked repetitive EPSCs in 33% of the granule cells tested in ipsilateral hippocampi from H-I-treated rats (4/12 granule cells, $p<0.02$, Fisher's exact test, n=6 rats). Contralateral hippocampi were not examined in this experiment. These data imply that the ipsilateral hippocampi following H-I treatment have a significant increase in new recurrent excitatory synapses.

Spontaneous motor seizures and Timm stain

After the H-I injury, all rats were observed in the vivarium for 6–18 months to detect subsequent epileptic seizures. Two spontaneous motor seizures were observed per rat in 3 out of 20 lesioned animals (15%, a total of 6 seizures in 3 rats), and these 3 animals lived for 18 months after H-I. The spontaneous motor seizures were not observed until 6 months after H-I treatment (Fig. 9A), with a seizure rate that was relatively low (0.0043 seizures/h, or approximately 1 seizure every 10 days). The number of days to the first observed seizure (based on 6 h of weekly monitoring) for the H-I rats was 285 ± 91 days. These data suggest that this model of brain injury can induce epilepsy in at least a small percentage of animals after a latent period, but continuous monitoring is required to assess the issue of a latent period.

A further analysis of the Timm-stain data consisted of placing the lesioned hippocampi into separate groups, depending on whether or not the animals were seen to have spontaneous motor seizures (Fig. 9B). The rats that did demonstrate spontaneous motor seizures had significantly more Timm stain in the inner molecular layer of both the ipsilateral and contralateral hippocampi compared to the H-I rats with no seizures ($p<0.05$, Kruskal-Wallis). The ipsilateral hippocampus from the rats with seizures also had significantly elevated amounts of Timm stain in the inner molecular layer compared to the contralateral hippocampi from the animals with seizures ($p<0.05$, Kruskal-Wallis).

DISCUSSION

Overview of results

The goal of this study was to test the hypothesis that the neuronal loss caused by an H-I injury at 30 days of age would be associated with synaptic reorganization in the hippocampus over the subsequent several months, and that these new local excitatory circuits would lead to abnormal electrophysiological responses (i.e., all-or-none burst discharges) in the dentate gyrus. In the present study, neuron loss was observed in the hilus and CA1 area of the ipsilateral dorsal hippocampus. Timm stain in the IML (i.e., mossy fiber sprouting) was mild to moderate,

and occurred in the dorsal region of both ipsilateral and contralateral hippocampi. In normal medium, hippocampal slices showed electrophysiological responses to stimulation of the hilus that were relatively normal. When challenged with bicuculline and 6 mM $[K^+]_o$, however, slices from the experimental group were far more likely to generate all-or-none burst responses to hilar stimulation than slices from control animals. Behavior of the rats was monitored 6 h/week for up to 18 months, and 15% were observed to have chronic spontaneous motor seizures. Those animals with motor seizures had more Timm staining in the IML. These studies suggest a possible linkage between neuronal loss, synaptic reorganization leading to the formation of new recurrent excitatory circuits, and the presence of spontaneous seizures; however, additional studies are needed to test this general hypothesis, and specifically to determine whether the hippocampus plays a role in the generation of the seizures.

The H-I model in 30-day-old rats

Ischemic brain injury in humans has a highly variable clinical presentation, anatomic location and etiology; and therefore, no single rodent model of ischemic brain injury can adequately reproduce the human injury in all of its diversity. The animal model that is most commonly used to study global forebrain ischemia is the four-vessel occlusion model, which causes hippocampal injury but does not consistently generate a gross and histological lesion in the neocortex. Occlusion of the middle cerebral artery or photothrombotic-induced injury leads to both gross and histopathological injury in the neocortex, but the hippocampus is spared (for a full review of the models see Ginsberg and Busto, 1989). None of the above models have demonstrated chronic spontaneous motor seizures, although electrographic abnormalities have been seen (Kelly et al., 2001; Kelly, 2002; Karhunen et al. 2003, 2006; Epsztein et al., 2006). These observations led to the hypothesis that both hippocampal and neocortical injury may potentiate the generation of chronic motor seizures in rodents. Based on previous work (Towfighi et al., 1997; Towfighi and Mauger, 1998) and our experience with the H-I model in perinatal rats (Williams et al. 2004), we chose the H-I injury model in 30-day-old rats because it was expected that this animal model would consistently have unilateral hippocampal and neocortical injury. Although the injury caused by this model is not a true ischemia, the pattern of hippocampal neuronal loss, as discussed below, is suggestive of common mechanisms. The current study did not investigate the neocortical injury beyond a gross anatomic description. We chose to focus on the hippocampal injury, because it has been well characterized in numerous models of epilepsy. This has allowed us to address hypotheses concerning axonal sprouting as a marker of epilepsy and as an indication of the formation of new recurrent excitatory synapses, which may well be present in peri-lesional sites throughout the injured hemisphere.

Pattern of neuron loss

An important feature of this model is that the H-I treatment has been shown to cause dramatic neuronal loss in the ipsilateral (i.e., unilateral) fronto-parietal cortex and dorsal hippocampus (Towfighi et al., 1997; Towfighi and Mauger, 1998); similar results were obtained in this study. The present study expands on previous work by using the optical fractionator method to quantify hippocampal neuronal loss along the septo-temporal axis of the hippocampus. Our rationale for a quantitative examination of hippocampal neuronal loss was to: (1) verify that the H-I procedure successfully induced a brain injury, and (2) examine the association between neuronal loss and mossy fiber sprouting, which showed a significant correlation in this model. The pattern of hippocampal neuron loss after a 30-day H-I lesion is similar to the pattern seen in humans after global forebrain ischemia and in adult rats using the four-vessel occlusion model, which involves preferential loss of CA1 pyramidal neurons and hilar neurons with relative sparing of the CA3 neurons and the granule cells (Pulsinelli and Brierley, 1979, Pulsinelli et al., 1982, Petito et al., 1987). As shown by Towfighi et al. (1997), the pattern of hippocampal neuron susceptibility shifts from area CA3 after H-I injury in postnatal day 7 (P7)

rats to area CA1 and the hilus in rats given the H-I treatment at P30. In humans and animal models of temporal lobe epilepsy, hippocampal neuron loss typically involves hilar neuron loss with injury to both CA3 and CA1 (Babb and Brown, 1987; Franck and Roberts, 1990); thus, the lesions commonly observed in temporal lobe epilepsy could be viewed to be a mixture of the lesions seen in both the P7 and P30 H-I animals. While different initiating mechanisms (i.e. relative oligemia versus global ischemia versus status epilepticus) cause the neuronal loss in the various models, the similarities in neuronal vulnerability argue for a convergence of the mechanisms responsible for neuronal death (e.g., excitatory amino acid neurotoxicity, Olney, 1980). The consequences of hilar neuron loss after an H-I insult at P30, and the alterations that occur over the next several months in the local circuitry, were the primary focus of the experiments in the present study.

The hilus contains a heterogenous population of neurons (Amaral, 1978), and hilar neuron loss seen in the models of temporal lobe epilepsy represents loss of both glutamatergic (e.g., mossy cells, Scharfman et al., 2001) and GABAergic interneurons (e.g., parvalbumin and somatostatin containing neurons, Buckmaster and Dudek, 1997b), with a similar pattern of hilar neuron loss seen after global forebrain ischemia in the rat four-vessel occlusion model (Hsu and Buzsaki, 1993; Schmidt-Kastner and Hossmann, 1998; Arabadzisz and Freund, 1999). The type of hilar neuron loss seen in the 30-day H-I model is currently unknown. Inhibitory transmission in the dentate gyrus appears to be decreased in rat models of temporal lobe epilepsy (Kobayashi and Buckmaster, 2003; Cohen et al., 2003; Shao and Dudek, 2005), while dentate inhibition appeared normal with no hyperexcitable responses many months after global forebrain ischemia in rats (Mody et al., 1995). Although not the focus of the present study, electrophysiologic experiments on hippocampal slices from P30 H-I rats several months after the H-I injury suggested that inhibition was not dramatically depressed, since no abnormal responses were seen in hippocampal slices from H-I rats to hilar stimulation in normal medium, and abnormal responses were not seen until after the application of bicuculline.

Role of hilar neuron loss in mossy fiber sprouting

Hilar neuron loss may be an initiating factor that leads to mossy fiber sprouting (e.g., Dudek and Spitz, 1997); loss of excitatory input from mossy cells onto granule cell dendrites in the inner molecular layer may stimulate granule cells to sprout new mossy fiber axons to replace the lost synapses. Based on this hypothesis, severe hilar neuron loss would be predicted to lead to robust mossy fiber sprouting. The relatively weak Timm stain in the IML (i.e., mossy fiber sprouting) of the ipsilateral hippocampus in the 30-day H-I model and the presence of mossy fiber sprouting in the contralateral hippocampus suggest that hilar neuron loss may not be the main cellular mechanism driving the formation of new recurrent excitatory synapses. One possible explanation is that the relative preservation of the temporal hilus and mossy cell axonal arborization along the septo-temporal axis (Buckmaster et al., 1996) may prevent extensive loss of excitatory synapses on granule cells in the IML of the septal hippocampus. These data also suggest factors other than neuronal loss may be important in the initiation and generation of robust mossy fiber sprouting, which may include growth factors (for a review see Jankowsky and Patterson, 2001), interictal spikes, and potentially seizures themselves (Staley et al., 2006).

Mossy fiber sprouting and spontaneous seizures

The animals that had been observed to have spontaneous seizures also had the greatest amount of Timm stain in the inner molecular layer (i.e., based on highest scores using the scale of Tauck and Nadler (1985)). Several studies using the kainate and pilocarpine models have reported that animals with spontaneous seizures consistently have Timm stain in the IML, but the frequency and the properties of the seizures do not usually correlate with the density or robustness of the sprouting (Buckmaster and Dudek, 1999; Pitkanen et al., 2000). Reasons for this lack of correlation probably include but are not limited to the multifactorial nature of the

epileptogenic process, the need to record electrographic seizures from the specific area under study, and the probable participation of numerous brain areas in seizures (even relatively focal seizures). The dentate gyrus and hippocampus represent a relatively simplified model of other cortical regions where neuron loss and axon sprouting are also likely to be cellular mechanisms associated with brain injury.

Contralateral hippocampus

A “mirror focus” occurs when a primary seizure-generating area causes formation of a secondary focus in the homotopic contralateral cortex (Morrell et al., 1993); this can be induced experimentally by creating a focal lesion in one cortical hemisphere. Electrographic recordings from both the lesioned site and its homotopic contralateral site have shown that seizure-like activity initially arises from the lesioned site and is typically followed over time by seizure activity in the homotopic contralateral site. Seizure-like activity in the secondary site continues even after removal of the primary lesioned focus (Morrell et al., 1993). It has been hypothesized that deafferentation of the homotopic cortex may lead to epileptogenesis at this secondary site through axonal sprouting and synaptic reorganization (Dudek and Spitz, 1997). Electrophysiological abnormalities have been demonstrated in the contralateral somatosensory cortex (i.e., diaschisis) of the rat 7 days after a photothrombotic lesion to the ipsilateral somatosensory cortex (Buchrehmer-Ratzman et al., 1996). Hilar neurons, especially the mossy cells, have extensive commissural input to the IML of the contralateral hippocampus (Blackstad, 1956; Frotscher et al., 1981; Seress and Ribak, 1984; Frotscher and Zimmer, 1987), and mossy cells are damaged or killed during global ischemia (Hsu and Buzsaki, 1993). Neuron loss was not detected in the contralateral CA1 area or the hilus, as determined by the optical fractionator method, but the contralateral hemisphere could have been affected by the H-I treatment, since it was exposed to hypoxic conditions. The alterations in the contralateral hippocampus may have arisen because these animals experienced global hypoxia (8% oxygen for 30 min), although this explanation seems unlikely because hypoxia alone (6% oxygen) at 10–12 days of age (Jensen, 1995) does not show neuron loss, mossy fiber sprouting, or spontaneous seizures. Therefore, it is unlikely that 8% hypoxia alone can account for the mossy fiber sprouting that is present in the H-I model when the procedure is performed in either 7- (Williams et al., 2005) or 30-day-old rats. The altered electrophysiologic responses in the contralateral hippocampi may be in part due to the presence of new recurrent excitatory circuits, because the ipsilateral loss of hilar neurons may lead to deafferentation of the contralateral granule cell layer and subsequent mossy fiber sprouting.

Evidence for new recurrent excitatory circuits

One important question concerning the histopathological observation of increased Timm stain in the inner molecular layer is whether these anatomical changes are associated with physiologically relevant alterations in neuronal circuitry. These histopathological alterations were not associated with obvious “hyperexcitability” in normal medium, and studies using the four-vessel occlusion model have not reported hippocampal “hyperexcitability” shortly after or many months after global ischemia in normal medium (Mody et al., 1995; Xu and Pulsinelli, 1996; Howard et al., 1998; Arabadzisz et al., 2002). Congar and coworkers (2000), however, have reported that the CA3 region has a lower seizure threshold, and Epszstein and colleagues (2006) showed that this region produces abnormal interictal activity many months after global ischemia. Previous work with the kainate, pilocarpine and kindling models in several laboratories (e.g., Cronin et al., 1992; Wuarin and Dudek, 1996, 2001; Patrylo and Dudek, 1998; Lynch and Sutula, 2000; Hardison et al., 2000) all point to the idea that alterations in local excitatory circuits are masked by inhibitory circuits, and pharmacological depression of $GABA_A$-receptor-mediated inhibition and/or increased $[K^+]_o$ unmask the abnormalities. This concept is based on early work in the CA3 area of normal animals, where depression of inhibition unmasked the presence of recurrent excitation (Miles and Wong, 1987; Christian

and Dudek, 1988a, b). In a cortical network (e.g., hippocampus or neocortex) containing a population of principal neurons (e.g., pyramidal cells or granule cells) with many excitatory synaptic inputs from a population of afferent axons, where GABAergic inhibition has been blocked (and without recurrent excitation), small step-wise increases in stimulus intensity would be expected to recruit progressively more afferent axons and thus progressively activate more excitatory synapses on each of the principal neurons in the population, thus leading to synaptic responses where the amplitude is graded with the stimulus intensity (i.e., the response amplitude increases with each step-wise increase in stimulus intensity). A critical point is that with the same network configuration, but *in the presence of sufficient recurrent excitation, weak stimuli can activate the entire network*, but not necessarily in response to every stimulus. If a particular stimulus does not activate enough neurons or an appropriate group of principal cells, then the activity may not spread through the entire network. This is a fundamental property of a network with recurrent excitation, and leads to a condition where the responses are all-or-none and typically have long and variable latencies at low stimulus intensities, which arise from the long and variable pathways that the activity must propagate through the network of recurrent excitatory connections (Traub and Wong, 1982; Miles and Wong 1983; Miles and Wong, 1987). We used hilar stimulation because this would be expected to activate mossy fiber axons and potential recurrent excitatory circuits, whereas stimulation of the perforant path would activate powerful excitatory synapses from the entorhinal cortex. Hilar stimulation in bicuculline with 6 mM $[K^+]_o$ often caused all-or-none bursts in the slices from H-I rats but not control animals. All-or-none bursting was defined as bursts of population spikes with a distinct threshold. The hippocampal slices from P30 H-I rats produced all-or-none bursts of population spikes, but the prolonged after-discharges characteristic of some slices from rats with kainate-induced epilepsy (Wuarin and Dudek, 1996; Patrylo and Dudek, 1998) were rarely observed. The bursts generated from the H-I rats may have been less robust because the amount of Timm stain in the inner molecular layer of the H-I rats was less than was typically seen in kainate- and pilocarpine-treated rats. The electrophysiological differences of hippocampal slices from kainate- and pilocarpine-treated rats compared to H-I animals may also arise from inherent differences in septal hippocampal slices (i.e., H-I rats) versus the temporal hippocampus (i.e., kainate- and pilocarpine-treated rats). Differences between the septal and temporal hippocampus in the rate of kindling and frequency of spontaneous bursting in CA3 have suggested that the temporal hippocampus is more prone to epileptiform activity (Racine et al., 1977; Bragdon et al., 1986). Mechanisms other than mossy fiber sprouting in the IML and the formation of new recurrent excitatory synapses, such as the formation of new excitatory synapses with basilar dendrites (Ribak et al., 2000) and alterations in glutamate receptors (Mathern et al., 1996), could also contribute to the abnormal electrophysiological responses seen after H-I injury. It is possible that mossy cells in the hilus were activated with hilar stimulation, and that strong feed-forward inhibition from hilar interneurons largely masked this response. However, this condition is present in control animals, and our controls and controls from numerous other studies have never shown long bursts of all-or-none population spikes that are typically present in cell populations with a recurrent excitatory network. The mossy cell network may contribute to the graded response sometimes seen in control animals to electrical stimulation of the hilus. Furthermore, all mossy cell input would be associated with a field EPSP, which was not seen in slices from our controls or our experimental animals; thus, mossy cell input is not a likely explanation for the abnormal activity seen after a H-I injury at 30 days of age. Finally, the abnormal hippocampal activity manifest was not an actual seizure, but rather an all-or-none burst that probably – based on previous research cited above - reflects the “unmasking” of new recurrent excitatory circuits. The presence of Timm stain in the inner molecular layer (i.e., mossy fiber sprouting) should be viewed as one marker for temporal lobe epilepsy associated with mesial temporal sclerosis, and likely one of several abnormal networks that may increase the probability of seizure generation. The relationship between the presence of new recurrent excitatory synapses and the occurrence of spontaneous

motor seizures is unlikely direct, particularly since alterations in inhibitory circuits are likely and presumably play a role in the unmasking of recurrent excitation.

Focal flash photolysis of caged glutamate has many advantages for mapping local neuronal circuitry (Callaway and Katz, 1993; Katz and Dalva, 1994; Dalva and Katz, 1994). Focal activation of the soma-dendritic region of dentate granule cells with glutamate microdrops or photo-stimulation of caged glutamate could evoke EPSCs in recorded granule cells in tissue from kainate-and pilocarpine-treated rats (Wuarin and Dudek, 1996; Molnar and Nadler, 1999; Lynch and Sutula, 2000). The results reported here are similar to the data of Wuarin and Dudek (2001) in which slices from kainate-treated rats 2–4 weeks after kainate treatment showed moderate Timm stain in the inner molecular layer with a small but significant number of granule cells (32%) that demonstrated granule cell-to-granule cell interactions. Thus, the present data with focal granule cell activation using photoactivation of caged glutamate is consistent with the data from electrical stimulation of the hilus that granule cells progressively form new recurrent excitatory circuits after an H-I insult at 30 days of age.

It has been suggested that the presence of mossy fiber sprouting in the inner molecular layer may be a marker of epilepsy (Gorter et al., 2000), and it may also serve as a marker of the formation of new recurrent excitatory circuits in other areas of the brain. Loss of excitatory input in other regions of the brain (e.g., contralateral dentate gyrus, CA1, subiculum, neocortex,) has also been proposed to lead to the formation of new recurrent excitatory circuits. Several lines of evidence argue that CA1 pyramidal cells form new recurrent excitatory synapses in rats with kainate-induced epilepsy, potentially in response to loss of excitatory input from CA3 (Perez et al., 1996; Meier and Dudek, 1996; Esclapez et al., 1999, Smith and Dudek, 2001, 2002; Shao and Dudek, 2004, 2005). A recent report by Epsztein et al. (2006) suggests that CA3 may under go reorganization after global ischemia. These data provide further support for the concept that formation of new recurrent excitatory circuits may be a widespread phenomenon after brain injury, and that abnormal Timm stain in the dentate gyrus is only one example of this form of synaptic reorganization.

Epilepsy

The most common cause of epilepsy in the elderly is stroke; the incidence of epilepsy after a stroke is 2–17% (Pohlmann-Eden et al., 1996; Olsen, 2001). The occurrence of epilepsy after stroke in humans closely matches the results observed in this model of H-I. Most patients with post-stroke epilepsy demonstrate lesions in the neocortex and have focal cortical injuries that are typically due to an ischemic accident in the middle cerebral artery (Berges et al., 2000). In this type of injury, the hippocampus is not usually involved. Hippocampal post-stroke injury in humans is usually caused by a unilateral or bilateral ischemic incident in the posterior cerebral artery, and is strongly associated with the clinical condition of post-stroke amnesia (Ott and Saver, 1993). This injury often involves the thalamus and portions of the amygdala and striatum, and seizures have not been reported in these cases, although that does not mean they do not occur. Global ischemia following cardiopulmonary arrest in humans is not widely reported to have an association with epilepsy, however, as improvements are made in the treatment and care of resuscitated patients, the appearance of chronic seizures may be a condition that becomes apparent. Regular monitoring of motor seizures was undertaken in all of the animals from the time of treatment until death or euthanasia, although the amount of monitoring was quite limited, which may account for the low proportion of H-I animals with spontaneous seizures. Previous studies using H-I models have generally failed to report seizures many months after these types of treatments, but this may have been due to the low seizure rate. In the study of Romijn and coworkers (1994), 5-sec electrophysiological abnormalities were observed, but it is not clear that these events meet the electrophysiological definition of a seizure (e.g., Zhang et al., 2002). Electrographic seizures have been reported in

aged animals months following a photothrombotic lesion (Kelly et al., 2001; Kelly, 2002). Chronic spontaneous motor seizures have generally not been identified in other stroke models (Karhunen et al. 2003, 2006). Though recently it has been reported by Karhunen et al. (2007) that rats do develop motor seizures after a cortical photothrombotic lesion in a proportion of animals similar to what was observed in this study. Acute seizures may develop immediately after head trauma or global ischemia (Pulsinelli and Brierley, 1979), but these seizures are typically not classified as epileptic in nature, because they usually do not persist beyond 1 week after the injury, and likely have different underlying mechanisms. The H-I animals had a substantially lower seizure rate than rats with kainate- or pilocarpine-induced epilepsy. Many people with epilepsy have low seizure rates, and this model recapitulates that abnormality in behavior. This could be in part due to the relatively unilateral nature of the lesion, since rats that receive unilateral intrahippocampal kainate injections also have low seizure rates in spite of bilateral abnormalities in Timm staining (Bragin et al., 1999).

Latent period

One concern relates to the interpretation of the data on the apparent latent period. In this study, the H-I rats were observed for 6 h per week until euthanized for slice electrophysiology experiments. This rate of observation only covers 4% of the possible time when a rat may display a seizure, which would be expected to overestimate the true latent period (i.e. the true latent period is presumably much shorter than presented here). In the current study, the main focus was to determine any evidence of epilepsy and synaptic reorganization. These data show that some animals develop spontaneous motor seizures several months after H-I treatment at postnatal day 30, and future studies should further investigate chronic recurrent seizures after H-I injury in 30-day-old animals.

Conclusion

The pattern of hippocampal neuron loss in this model of H-I in 30-day-old rats is similar to humans after global ischemia. Like animal models of temporal lobe epilepsy based on chemoconvulsant-induced status epilepticus, synaptic reorganization and formation of new recurrent excitatory circuits may contribute to the generation of the seizures. Mossy fiber sprouting was present not only in the lesioned hemisphere, but also in the unlesioned hemisphere, which could potentially be a marker for the formation of a secondary site of epileptogenesis. In terms of the development of chronic epilepsy, the 30-day H-I model appears to lead to a low fraction of animals with chronic epilepsy having a low seizure rate, similar to what is seen in the human population following a stroke, although more monitoring is needed to address this issue. That this model of H-I injury in young adult rats leads to epilepsy, at least in some animals, while motor seizures have not yet been demonstrated in other models of ischemic brain injury may indicate that a combination of factors (e.g., both neocortical and hippocampal injury, mossy fiber sprouting, and other undetermined factors) need to be present for the expression of chronic recurrent motor seizures.

Acknowledgments

This research was supported by NIH grants NS10643 (PAW) and NS16683 (FED).

Abbreviations

H-I	Hypoxia-ischemia
IML	Inner molecular layer
P7	Perinatal day 7

References

1. Amaral DG. A golgi study of cell types in the hilar region of the hippocampus in the rat. J Comp Neurol 1978;182:851–914. [PubMed: 730852]
2. Arabadzisz D, Freund TF. Changes in excitatory and inhibitory circuits of the rat hippocampus 12–14 months after complete forebrain ischemia. Neuroscience 1999;92:27–45. [PubMed: 10392828]
3. Arabadzisz D, Ylinen A, Emri Z. Increased inter-spike intervals and fast after-hyperpolarization of action potentials in rat hippocampal pyramidal cells accompanied with altered calbindin immunoreactivity 10–12 months after global forebrain ischemia. Neurosci Lett 2002;331:103–106. [PubMed: 12361851]
4. Babb, TL.; Brown, WJ. Pathological findings in epilepsy. In: Engel, J., editor. Surgical Treatment of the Epilepsies. New York: Raven Press; 1987. p. 511-540.
5. Berges S, Moulin Berger E, Tatu L, Sablot D, Challier B, Rumbach L. Seizures and epilepsy following strokes: recurrence factors. Eur Neurol 2000;43:3–8. [PubMed: 10601801]
6. Blackstad TW. Commissural connections of the hippocampal region in the rat, with special reference to their mode of termination. J Comp Neurol 1956;105:417–537. [PubMed: 13385382]
7. Bragdon AC, Taylor DM, Wilson WA. Potassium-induced epileptiform activity in area CA3 varies markedly along the septaltemporal axis of the rat hippocampus. Brain Res 1986;378:169–173. [PubMed: 3742197]
8. Bragin A, Engle J jr, Wilson CL, Vizentin E, Mathern GW. Electrophysiological analysis of a chronic seizure model after unilateral hippocampal KA injection. Epilepsia 1999;40:1210–21. [PubMed: 10487183]
9. Buchrehmer-Ratzman I, August M, Hagemann G. Electrophysiological transcortical diaschisis after cortical photothrombosis in rat brain. Stroke 1996;27:1105–1111. [PubMed: 8650722]
10. Buckmaster PS, Dudek FE. Network properties of the dentate gyrus in epileptic rats with hilar neuron loss and granule cell axon reorganization. J Neurophysiol 1997a;77:2685–2696. [PubMed: 9163384]
11. Buckmaster PS, Dudek FE. Neuron loss, granule cell reorganization, and functional changes in the dentate gyrus of epileptic kainate-treated rats. J Comp Neurol 1997b;385:385–404. [PubMed: 9300766]
12. Buckmaster PS, Dudek FE. In vivo intracellular analysis of granule cell axon reorganization in epileptic rats. J Neurophysiol 1999;81:712–721. [PubMed: 10036272]
13. Buckmaster PS, Wenzel HJ, Kunkel DD, Schwartzkroin PA. Axon arbors and synaptic connections of hippocampal mossy cells in the rat in vivo. J Comp Neurol 1996;366:271–292. [PubMed: 8698887]
14. Callaway EM, Katz LC. Photostimulation using caged glutamate reveals functional circuitry in living brain slices. Proc Natl Acad Sci 1993;90:7661–7665. [PubMed: 7689225]
15. Christian EP, Dudek FE. Characteristics of local excitatory circuits studied with glutamate microapplication in the CA3 area of rat hippocampal slices. J Neurophysiol 1988a;59:90–109. [PubMed: 2893832]
16. Christian EP, Dudek FE. Electrophysiological evidence from glutamate microapplications of local excitatory circuits in the CA1 area of rat hippocampal slices. J Neurophysiol 1988b;59:110–123. [PubMed: 2893830]
17. Cohen AS, Lin DD, Quirk GL, Coulter DA. Dentate granule cell $GABA_A$ receptors in epileptic hippocampus: enhanced synaptic efficacy and altered pharmacology. Eur J Neurosci 2003;17:1607–1616. [PubMed: 12752378]
18. Congar P, Gaiarsa JL, Popovici T, Ben-Ari Y, Crepel V. Permanent reduction of seizure threshold in post-ischemic CA3 pyramidal neurons. J Neurophysiol 2000;83:2040–2046. [PubMed: 10758114]
19. Cronin J, Obenaus A, Houser CR, Dudek FE. Electrophysiology of dentate granule cells after kainate-induced synaptic reorganization of the mossy fibers. Brain Res 1992;573:305–310. [PubMed: 1504768]
20. Dalva MB, Katz LC. Rearrangements of synaptic connections in visual cortex revealed by laser photostimulation. Science 1994;265:255–258. [PubMed: 7912852]
21. Dudek FE, Spitz M. Hypothetical mechanisms for the cellular and neurophysiologic basis of secondary epileptogenesis: proposed role of synaptic reorganization. J Clin Neurophysiol 1997;14:90–101. [PubMed: 9165404]

22. Epsztein J, Milh M, Bihi RI, Jorguere I, Ben-Ari Y, Represa A, Crepel V. Ongoing epileptiform activity in the post-ischemic hippocampus is associated with a permanent shift of excitatory-inhibitory synaptic balance in CA3 pyramidal neurons. J Neurosci 2006;26:7082–7092. [PubMed: 16807337]

23. Esclapez M, Hirsch JC, Ben-Ari Y, Bernard C. Newly formed excitatory pathways provide a substrate for hyperexcitability in experimenetal temporal lobe epilepsy. J Comp Neurol 1999;408:449–460. [PubMed: 10340497]

24. Franck JE, Roberts DL. Combined kainate and ischemia produces mesial temporal sclerosis. Neurosci Lett 1990;118:159–163. [PubMed: 2274264]

25. Frotscher M, Nitsch C, Hassler R. Synaptic reorganization in the rabbit hippocampus after lesion of commisural afferents. Anat Embryol 1981;163:15–30. [PubMed: 7316220]

26. Frotscher M, Zimmer J. Commisural fibers terminate on non-pyramidal neurons in the guinea pig hippocampus - a combined golgi/EM degeneration study. Brain Res 1987;265:289–293. [PubMed: 6850332]

27. Ginsberg MD, Busto R. Rodent models of cerebral ischemia. Stroke 1989;20:1627–1642. [PubMed: 2688195]

28. Gorter JA, van Vliet EA, Aronica E, Lopes da Silva FH. Progression of spontaneous seizures after status epilepticus is associated with mossy fibre sprouting and extensive bilateral loss of hilar parvalbumin and somatostatin-immunoreactive neurons. Eur J Neurosci 2001;13:657–669. [PubMed: 11207801]

29. Hardison JL, Okazaki MM, Nadler JV. Modest increase in extracellular potassium unmasks effect of recurrent mossy fiber growth. J Neurophysiol 2000;84:2380–2389. [PubMed: 11067980]

30. Houser CR, Miyashiro JE, Swartz BE, Walsh GO, Rich JR, Delgado-Escueta AV. Altered patterns of dynorphin immunoreactivity suggest mossy fiber reorganization in human hippocampal epilepsy. J Neurosci 1990;10:267–282. [PubMed: 1688934]

31. Howard EM, Gao TM, Pulsinelli WA, Xu ZC. Electrophysiological changes of CA3 neurons and dentate granule cells following transient forebrain ischemia. Brain Res 1998;798:109–118. [PubMed: 9666096]

32. Hsu M, Buzsaki G. Vulnerability of mossy fiber targets in the rat hippocampus to forebrain ischemia. J Neurosci 1993;13:3964–3979. [PubMed: 8366355]

33. Jankowsky JL, Patterson PH. The role of cytokines and growth factors in seizures and their sequelae. Prog Neurobiol 2001;63:125–149. [PubMed: 11124444]

34. Jensen FE. An animal model of hypoxia-induced perinatal seizures. Ital J Neurol Sci 1995;16:59–68. [PubMed: 7642353]

35. Karhunen H, Pitkanen A, Virtanen T, Gureviciene I, Pussinen R, Ylinen A, Sivenius J, Nissinen J, Jolkkonen J. Long-term functional consequences of transient occlusion of the middle cerebral artery in rats: a 1-year follow-up of the development of epileptogenesis and memory impairment in relation to sensorimotor deficits. Epilepsy Res 2003;54:1–10. [PubMed: 12742590]

36. Karhunen H, Nissinen J, Sivenius J, Jolkkonen J, Pitkanen A. A long-term video-EEG and behavioral follow-up after endothelin-1 induced middle cerebral artery occlusion in rats. Epilepsy Res 2006;72:25–38. [PubMed: 16911865]

37. Karhunen H, Bezvenyuk Z, Nissinen J, Sivenius J, Jolkkonen J, Pitkanen A. Epileptogenesis after cortical photothrombotic brain lesion in rats. Neurosci. 2007 (Epub ahead of print).

38. Katz LC, Dalva MB. Scanning laser photostimulation: a new approach for analyzing brain circuits. J Neurosci Meth 1994;54:205–218.

39. Kelly KM, Kharlamov A, Hentosz TM, Kharlamova EA, Williamson JM, Bertram E 3rd, Kapur J, Armstrong DM. Photothrombotic brain infarction results in seizure activity in aging Fischer 344 and Sprague-Dawley rats. Epilepsy Res 2001;47:189–203. [PubMed: 11738927]

40. Kelly KM. Poststroke seizures and epilepsy: clinical studies and animal models. Epilepsy Curr 2002;2:173–177. [PubMed: 15309107]

41. Kobayashi M, Buckmaster PS. Reduced inhibition of dentate granule cells in a model of temporal lobe epilepsy. J Neurosci 2003;23:2440–2452. [PubMed: 12657704]

42. Lamy C, Domingo V, Semah F, Arquizan C, Trystram D, Coste J, Mas JL. Patent foramen ovale and atrial septal aneurysm study group. Early and late seizures after cryptogenic ischemic stroke in young adults. Neurology 2003;60:400–404. [PubMed: 12578918]
43. Levine S. Anoxic-ischemic encephalopathy in rats. Am J Pathol 1960;36:1–17. [PubMed: 14416289]
44. Lynch M, Sutula T. Recurrent excitatory connectivity in the dentate gyrus of kindled and kainic acid-treated rats. J Neurophysiol 2000;83:693–704. [PubMed: 10669485]
45. Mathern GW, Leite JP, Babb TL, Pretorius JK, Kuhlman PA, Mendoza D, Fried I, Sakamoto A, Assirati JA, Adelson PD, Peacock WJ. Aberrant hippocampal mossy fiber sprouting correlates with greater NMDAR2 recptor staining. Neuroreport 1996;7:1029–1035. [PubMed: 8804045]
46. Meier CL, Dudek FE. Spontaneous and stimulation-induced synchronized burst afterdischarges in the isolated CA1 of kainite-treated rats. J Neurophysiol 1996;76:2231–2239. [PubMed: 8899598]
47. Mello L, Cavalheiro E, Tan A, Kupfer W, Pretorius J, Babb T, Finch D. Circuit mechanisms of seizures in the pilocarpine model of chronic epilepsy: Cell loss and mossy fiber sprouting. Epilepsia 1993;34:985–995. [PubMed: 7694849]
48. Miles R, Wong RKS. Single neurones can initiate synchronized population discharge in the hippocampus. Nature 1983;306:371–373. [PubMed: 6316152]
49. Miles R, Wong RKS. Inhibitory control of local excitatory circuits in the guinea pig hippocampus. J Physiol 1987;388:611–629. [PubMed: 3656200]
50. Mody I, Otis TS, Bragin A, Hsu M, Buzsaki G. Gabaergic inhibition of granule cells and hilar neuronal synchrony following ischemia-induced hilar neuronal loss. Neuroscience 1995;69:139–150. [PubMed: 8637612]
51. Molnar P, Nadler JV. Mossy fiber-granule cell synapses in the normal and epileptic rat dentate gyrus studied with minimal laser stimulation. J Neurophysiol 1999;82:1883–1894. [PubMed: 10515977]
52. Morrell, F.; Smith, MC.; deToledo-Morrell, L. Secondary epileptogenesis and kindling. In: Wyllie, E., editor. The Treatment of Epilepsy: Principle and Practice. Philadelphia: Lea and Febiger; 1993. p. 126-144.
53. Nadler JV, Perry BW, Cotman CW. Selective reinnervation of hippocampal area CA1 and the fascia dentata after destruction of CA3-CA4 afferents with kainic acid. Brain Res 1980;182:1–9. [PubMed: 7350980]
54. Olney JW. Excitatory amino acid neurotoxins: selectivity, specificity and mechanisms of action. II. Historical perspective. Neurosci Res Program Bulletin 1981;19:337–346.
55. Olsen TS. Post-stroke epilepsy. Curr Atheroscler Rep 2001;3:340–344. [PubMed: 11389801]
56. Onodera H, Aoki H, Yae T, Kogura K. Post-ischemic synaptic plasticity in the rat hippocampus after long-term survival: histochemical and autoradiographic study. Neuroscience 1990;38:125–136. [PubMed: 1701523]
57. Ott BR, Saver JL. Unilateral amnesic stroke. Six new cases and a review of literature. Stroke 1993;24:1033–42. [PubMed: 8322379]
58. Patrylo PR, Dudek FE. Physiological unmasking of new glutamatergic pathways in the dentate gyrus of hippocampal slices from epileptic kainate-treated rats. J Neurophysiol 1998;79:418–429. [PubMed: 9425210]
59. Perez Y, Morin F, Beaulieu C, Lacaille J-C. Axonal sprouting of CA1 pyramidal cells in hyperexcitable hippocampal slices of kainate-treated rats. Eur J Neurosci 1996;8:736–748. [PubMed: 9081625]
60. Petito CK, Feldmann E, Pulsinelli WA, Plum F. Delayed hippocampal damage in humans following cardiorespiratory arrest. Neurology 1987;37:1281–1287. [PubMed: 3614648]
61. Pitkanen A, Tuunanen J, Kalviainen R, Partanen K, Salmenpera T. Amygdala damage in experimental and human temporal lobe epilepsy. Epilepsy Res 1998;32:233–253. [PubMed: 9761324]
62. Pitkanen A, Nissinen J, Lakasiuk K, Jutila L, Paljarvi L, Salmenpera T, Karkola K, Vapalahti M, Ylinen A. Association between density of mossy fiber sprouting and seizure frequency in experimental and human temporal lobe epilepsy. Epilepsia 2000;41:524–529.
63. Pohlmann-Eden B, Hoch DB, Cochius JI, Henmeric MG. Stroke and epilepsy: Critical review of the literature part 1. Cerebrovasc Dis 1996;6:332–338.

64. Pulsinelli WA, Brierley JB. A new model of bilateral hemispheric ischemia in the unanesthetized rat. Stroke 1979;10:267–272. [PubMed: 37614]

65. Pulsinelli WA, Brierley JB, Plum F. Temporal profile of neuronal damage in a model of transient forebrain ischemia. Ann Neurol 1982;11:491–498. [PubMed: 7103425]

66. Racine RJ. Modification of seizure activity by electrical stimulation. II. Motor Seizure. Electroenceph Clin Neurophysiol 1972;32:281–294. [PubMed: 4110397]

67. Racine RJ, Rose PA, Burnham WM. Afterdischarge thresholds and kindling rates in dorsal and ventral hippocampus and dentate gyrus. Can J Neurol Sci 1977;4:273–278. [PubMed: 597802]

68. Ribak CE, Tran PH, Spigelman I, Okazaki MM, Nadler JV. Status epilepticus-induced hilar basal dendrites on rodent granule cells contribute to recurrent excitatory circuitry. J Comp Neurol 2000;428:240–253. [PubMed: 11064364]

69. Rice JE, Vannucci RC, Brierley JB. The influence of immaturity on hypoxic-ischemic brain damage. Ann Neurol 1981;9:131–141. [PubMed: 7235629]

70. Romijn HJ, Voskuyl RA, Coenen AML. Hypoxic-ischemic encephalopathy sustained in early post-natal life may result in permanent epileptic activity and an altered cortical convulsive threshold in rat. Epilepsy Res 1994;17:31–42. [PubMed: 8174523]

71. Scharfman HE, Smith KL, Goodman JH, Sollas AL. Survival of dentate hilar mossy cells after pilocarpine-induced seizures and their synchronized burst discharges with area CA3 pyramidal cells. Neuroscience 2001;104:741–759. [PubMed: 11440806]

72. Schmidt-Kastner R, Hossman K-A. Distribution of ischemic neuronal damage in the dorsal hippocampus of the rat. Acta Neuropath 1998;76:411–421. [PubMed: 2459897]

73. Seress L, Ribak CE. Direct commissural connections to basket cells of the hippocampal dentate gyrus: anatomic evidence for feedforward inhibition. J Neurocytol 1984;13:215–225. [PubMed: 6726288]

74. Shao LR, Dudek FE. Increased excitatory synaptic activity and local connectivity of hippocampal CA1 pyramidal cells in rats with kainate-induced epilepsy. J Neurophysiol 2004;92:1366–1373. [PubMed: 15084640]

75. Shao LR, Dudek FE. Detection of increased local excitatory circuits in the hippocampus during epileptogenesis using focal flash photolysis of caged glutamate. Epilpesia 2005;46(Suppl 5):100–106.

76. Shao LR, Dudek FE. Changes in mIPSCs and sIPSCs after kainate treatment: evidence for loss of inhibitory input to dentate granule cells and possible compensatory responses. J Neurophysiol 2005;94:952–960. [PubMed: 15772233]

77. Shetty AK, Turner DA. Fetal hippocampal cells grafted to kainate-lesioned CA3 region of adult hippocampus suppress aberrant supragranular sprouting of host mossy fibers. Exp Neurol 1997;143:231–245. [PubMed: 9056386]

78. Smith BN, Dudek FE. Short- and long-term changes in CA1 network excitability after kainate treatment in rats. J Neurophysiol 2001;85:1–9. [PubMed: 11152700]

79. Smith BN, Dudek FE. Network interactions mediated by new excitatory connections between CA1 pyramidal cells in rats with kainate-induced epilepsy. J Neurophysiol 2002;87:1655–1658. [PubMed: 11877537]

80. Staley K, Hellier JL, Dudek FE. Do interictal spikes drive epileptogenesis? Neuroscientist 2005;11:272–276. [PubMed: 16061513]

81. Tauck DL, Nadler JV. Evidence of functional mossy fiber sprouting in hippocampal formation of kainic acid-treated rats. J Neurosci 1985;5:1016–1022. [PubMed: 3981241]

82. Towfighi J, Maugher D, Vannucci RC, Vannucci SJ. Influence of age on the cerebral lesion in an immature rat model of cerebral hypoxia-ischemia: a light microscopic study. Devel Brain Res 1997;100:149–160. [PubMed: 9205806]

83. Towfighi J, Mauger D. Temporal evolution of neuronal changes in cerebral hypoxia-ischemia in developing rats: a quantitative light microscopic study. Dev Brain Res 1998;109:169–177. [PubMed: 9729365]

84. Traub RD, Wong RKS. Cellular mechanism of neuronal synchronization in epilepsy. Science 1982;216:745–747. [PubMed: 7079735]

85. West MJ, Slomianka L, Gunderson HJG. Unbiased stereological estimation of the total number of neurons in the subdivisions of the rat hippocampus using the optical fractionator. Anat Rec 1991;231:482–497. [PubMed: 1793176]

86. Williams PA, Wuarin J-P, Dou P, Ferraro DJ, Dudek FE. A reassessment of cycloheximide on mossy fiber sprouting and epileptogenesis in the pilocarpine model of temporal lobe epilepsy. J Neurophysiol 2002;88:2075–2087. [PubMed: 12364529]

87. Williams PA, Pou P, Dudek FE. Epilepsy and synaptic reorganization in a model of perinatal hypoxia-ischemia. Epilepsia 2004;45:1210–1218. [PubMed: 15461675]

88. Wuarin JP, Dudek FE. Electrographic seizures and new recurrent excitatory circuits in the dentate gyrus of hippocampal slices from kainate-treated epileptic rat. J Neurosci 1996;16:4438–4448. [PubMed: 8699254]

89. Wuarin J-P, Dudek FE. Evidence from whole-cell recordings and focal activation of caged glutamate that excitatory synaptic input to granule cells increases with time after kainate treatment. J Neurophysiol 2001;85:1067–1077. [PubMed: 11247977]

90. Xu ZC, Pulsinelli WA. Electrophysiological changes of CA1 pyramidal neurons following transient forebrain ischemia: an in vivo intracellular recording and staining study. J Neurophysiol 1996;76:1689–1697. [PubMed: 8890285]

91. Zhang X, Shu-sen C, Wallace AE, Hannesson DK, Schmued LC, Saucier DM, Honner WG, Corcoran ME. Relations between brain pathology and temporal lobe epilepsy. J Neurosci 2002;22:6052–6061. [PubMed: 12122066]

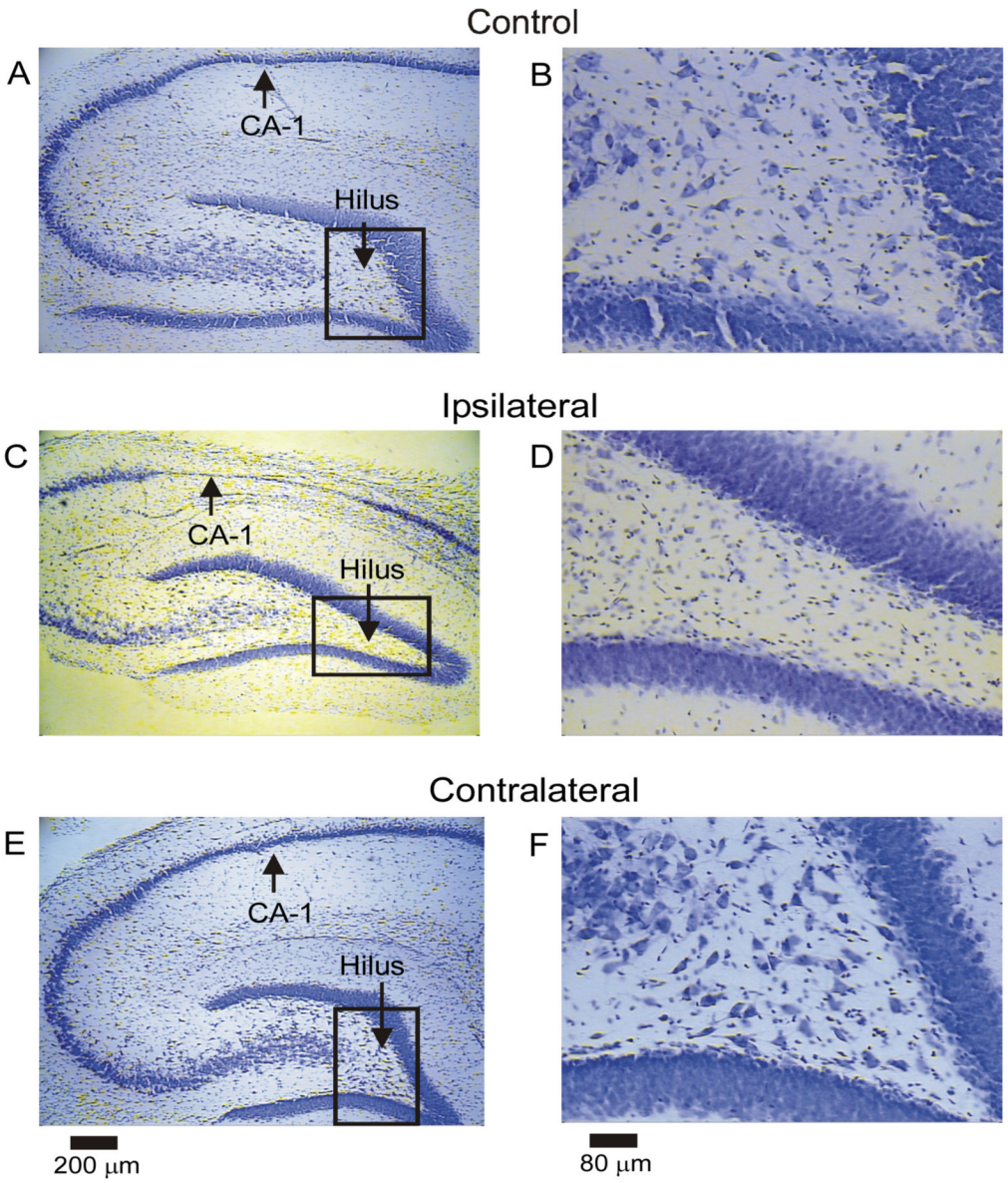

Figure 1.

Hippocampal neuron loss after H-I injury in the septal hippocampus. Low- and high-magnification micrographs (left and right respectively) of cresyl-violet stained sections are shown from a sham control rat (A, B), the ipsilateral hippocampus from an H-I rat (C, D), and the contralateral hippocampus from the same H-I animal (E, F). The hilus and CA1 of the ipsilateral hippocampus appeared most susceptible to H-I injury (panels C and D). Both the sham control and contralateral hippocampi did not show obvious neuron loss (panels A, B and E, F respectively).

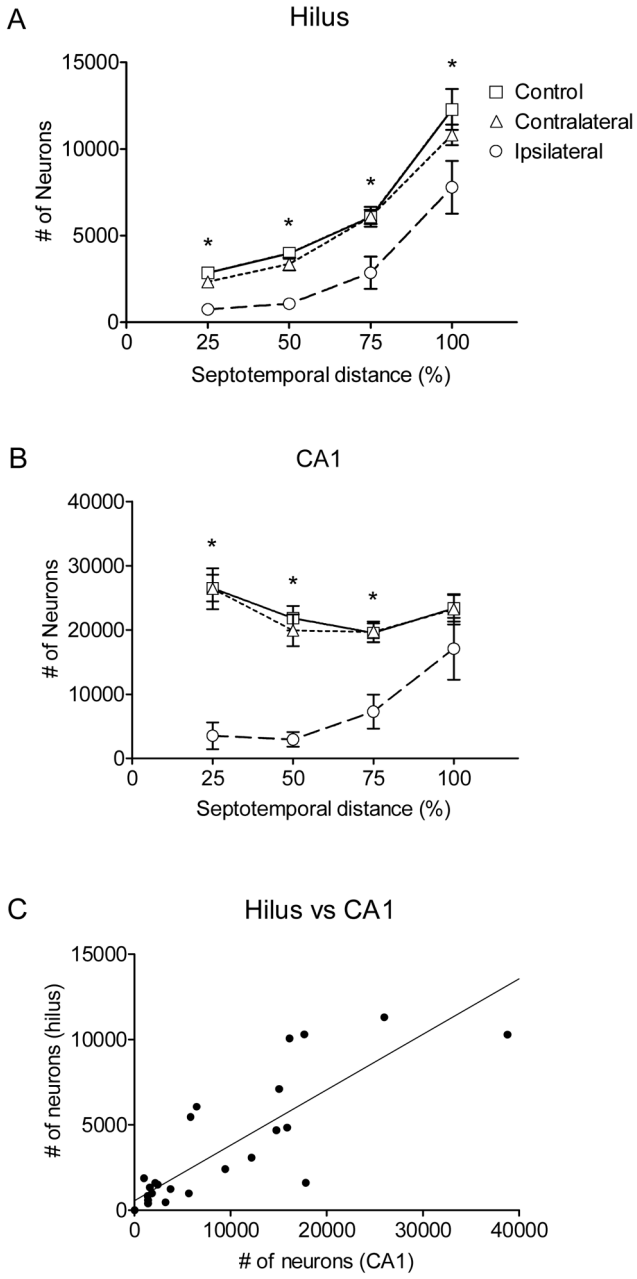

Figure 2.

Quantitative analysis of neuron loss along the septotemporal axis of the hippocampus after H-I injury. The ipsilateral hippocampus had significant neuron loss in the hilus (Panel A) throughout the septotemporal axis compared to both the sham control and the contralateral hippocampus ($p<0.01$. ANOVA, SNK, asterisks denote significant differences), except at the temporal end (100%), where the ipsilateral hippocampus was significantly different from the sham control ($p<0.05$, ANOVA, SNK), but not the contralateral hippocampus ($p>0.05$, ANOVA, SNK). The contralateral hippocampus did not have significant neuron loss compared to the sham control hippocampus ($p>0.05$, ANOVA, SNK). Total mean hilar neuronal counts were 11,120 ± 2,713 for the ipsilateral hippocampi; 22,224 ± 1,350 for the contralateral hippocampi, and 25,186 ± 1,608 for control hippocampi with a 56% reduction in hilar neurons

in ipsilateral hippocampi. The total mean counts for hilar neurons from ipsilateral hippocampi were significantly different from both contralateral and control hippocampi ($p<0.001$, ANOVA, SNK), while the total mean hilar counts for contralateral hippocampi were not signifantly different from controls ($p>0.05$, ANOVA, SNK). Severe pyramidal cell loss was apparent in the ipsilateral CA1 area of the septal hippocampus (25% and 50%), and neuron counts were significantly different ($p<0.001$, ANOVA, SNK, Panel B, asterisks denote significant differences) from both the sham control and contralateral hippocampus up to the temporal end (100%), where neuron counts in the ipsilateral hippocampus were not significantly different from either the sham control or the contralateral hippocampus ($p>0.05$, ANOVA, SNK). Total mean CA1 neuronal counts were 27,729 ± 8,539 for the ipsilateral hippocampi; 87,317 ± 7,773 for the contralateral hippocampi, and 91,218 ± 5,630 for control hippocampi with a 70% reduction in CA1 neurons in ipsilateral hippocampi. The total mean counts for CA1 neurons from ipsilateral hippocampi were significantly different from both contralateral and control hippocampi ($p<0.001$, ANOVA, SNK), while the total mean CA1 counts for contralateral hippocampi were not signifantly different from controls ($p>0.05$, ANOVA, SNK). Neuron counts in the hilus (Panel C) of the ipsilateral hippocampus were significantly correlated to CA1 neuron counts in the ipsilateral hippocampus ($r^2=0.71$, $p=0.0001$), suggesting that neuron loss in one area was associated with neuron loss in the other area.

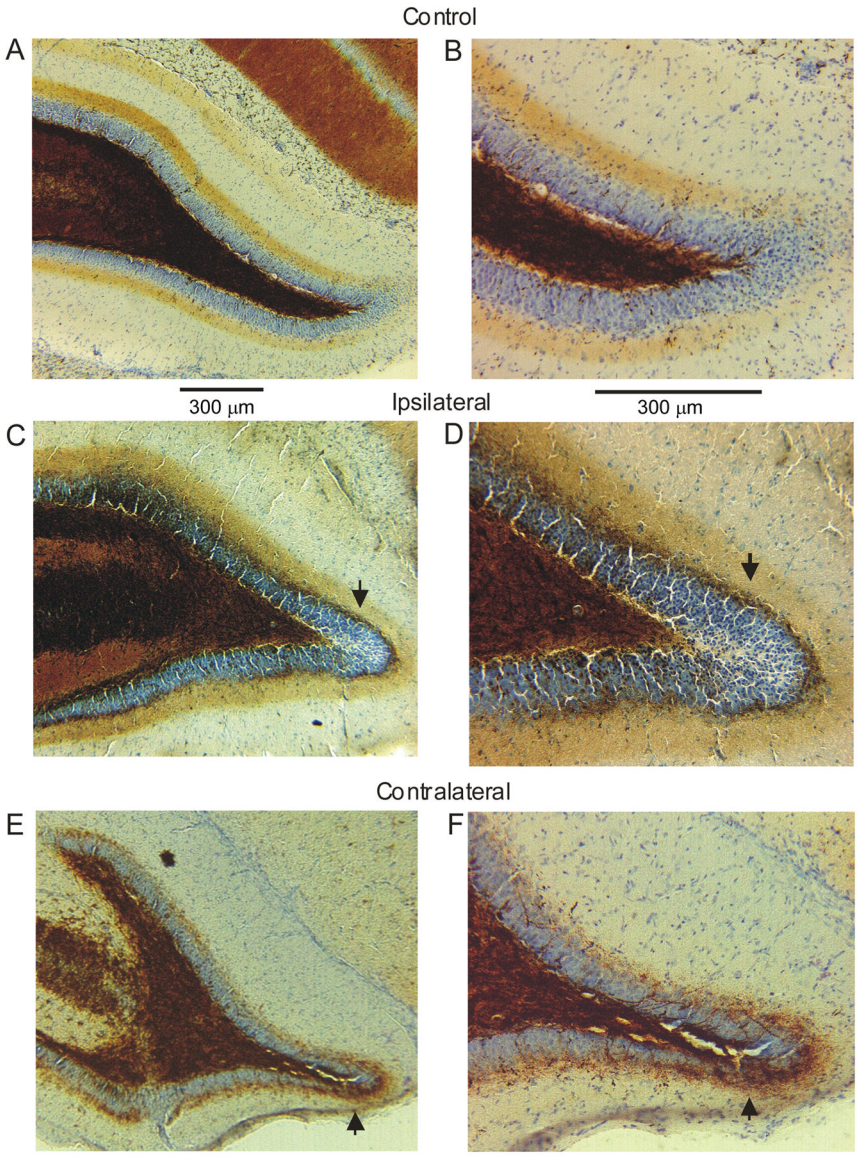

Figure 3.

Timm stain in the IML was assessed in both the ipsilateral and contralateral hippocampi of the H-I lesioned rats. No Timm stain was seen in the IML of the control hippocampi (A, B). Both the ipsilateral (C, D) and contralateral (E, F) hippocampi from H-I lesioned rats contained small-to-modest amounts of Timm stain in the IML (these would be scored as “2” and “1,” respectively, with the scale of Tauck and Nadler(1985)). Arrows point to abnormal Timm stain in the IML.

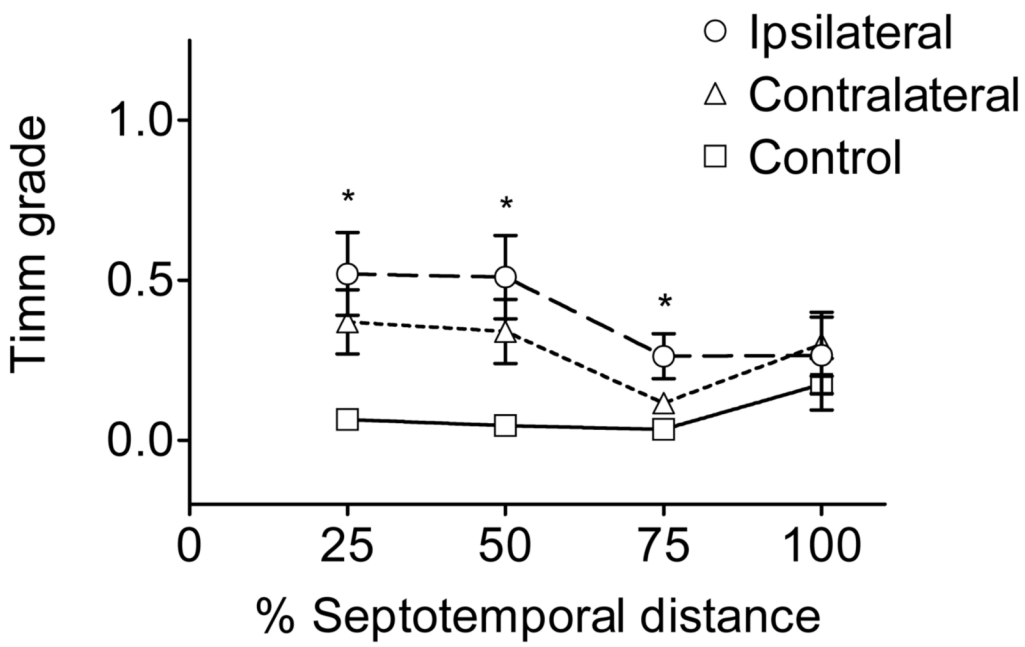

Figure 4.

Septotemporal analysis of Timm stain in the IML. The 25% region was defined as the septal end, the 100% region was defined as the temporal end, and each data point is an average Timm score. Timm stain in the IML of the ipsilateral hippocampi from lesioned animals was not robust, but significantly elevated in the septal and middle hippocampus (i.e., the 25%, 50% and 75% region of the hippocampus, marked by asterisks) as compared to the sham controls ($p<0.05$, Kruskal-Wallis; see Fig. 3A). A median score of 0.5 was obtained for all three regions of the ipsilateral hippocampus with a range of 0–2 for the Timm stain in the IML compared to a median score of 0 with a range of 0–0.5 for controls. The contralateral hippocampus had significantly elevated Timm stain in the IML compared to controls in the 25% and 50% hippocampal region ($p<0.05$, Kruskal-Wallis) with the same median and range as the ipsilateral hippocampus. Average scores are shown in the graph for ease of representation.

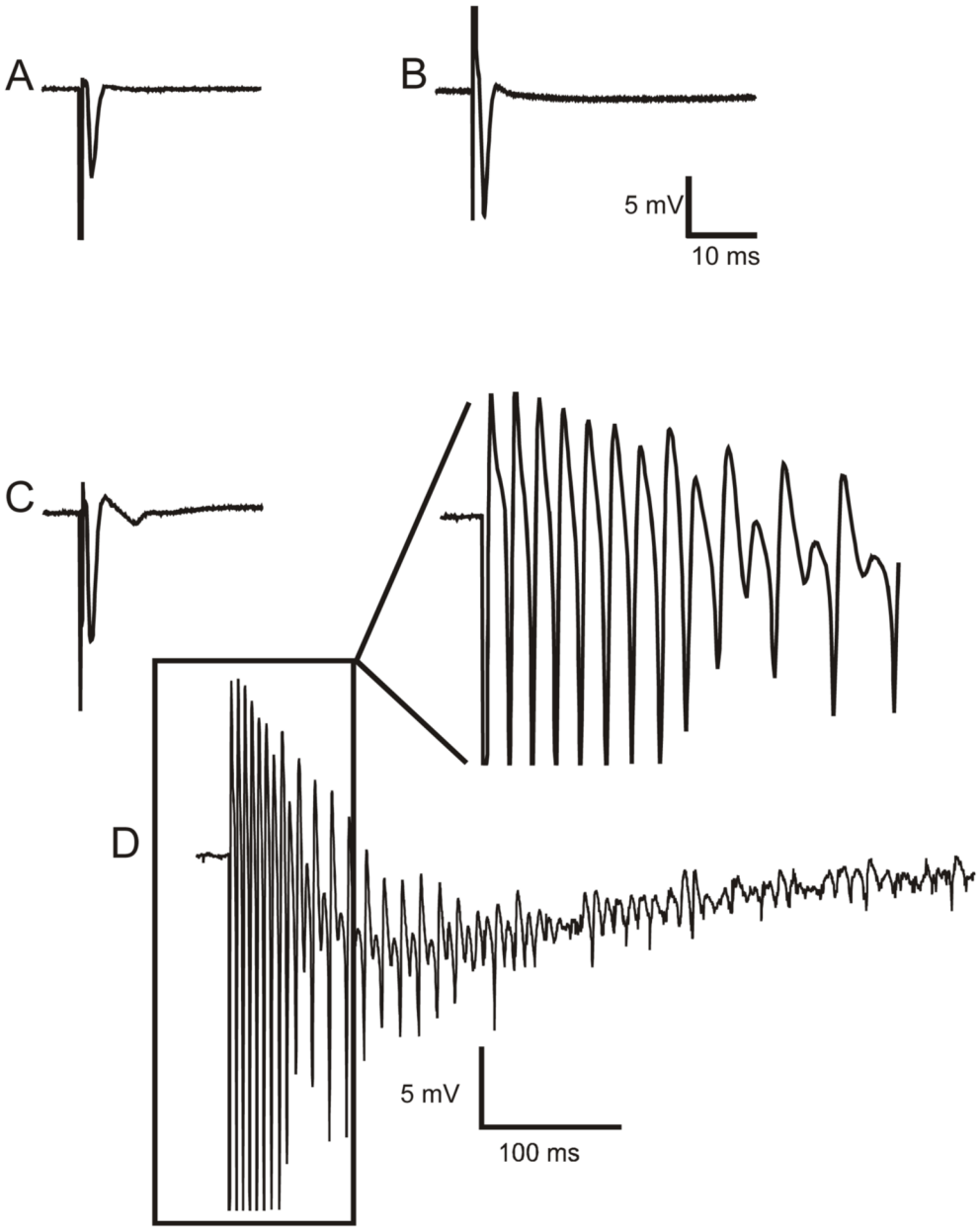

Figure 5.

Extracellular responses of dentate granule cells to hilar stimulation in a septal hippocampal slice bathed in either control solution or in ACSF containing elevated $[K^+]_o$ (6 mM) with 30 μM bicuculline. Panels A (slice from a control animal) and B (slice from the ipsilateral hippocampus of H-I treated animal) show antidromic responses from the granule cell layer to hilar stimulation in control solution. Panels C (control) and D (ipsilateral H-I) illustrate responses to hilar stimulation from the same recording site in ACSF containing 6 mM $[K^+]_o$ and 30 μM bicuculline. The field-potential responses of slices from control rats to hilar stimulation in 6 mM $[K^+]_o$ and 30 μM bicuculline showed either a single antidromic population spike, or occasionally, a small graded burst with a few population spikes (see Fig. 6). Several months after H-I treatment, hilar stimulation evoked a large burst of population spikes that

occurred in the ipsilateral hippocampus, which was only seen in slices from the experimental group in 6 mM $[K^+]_o$ and 30 μM bicuculline. All traces are averages of five responses, except for panel D, which shows a single trace. Stimulus artifacts have been reduced, and the initial population spike of the burst in panel D has been clipped.

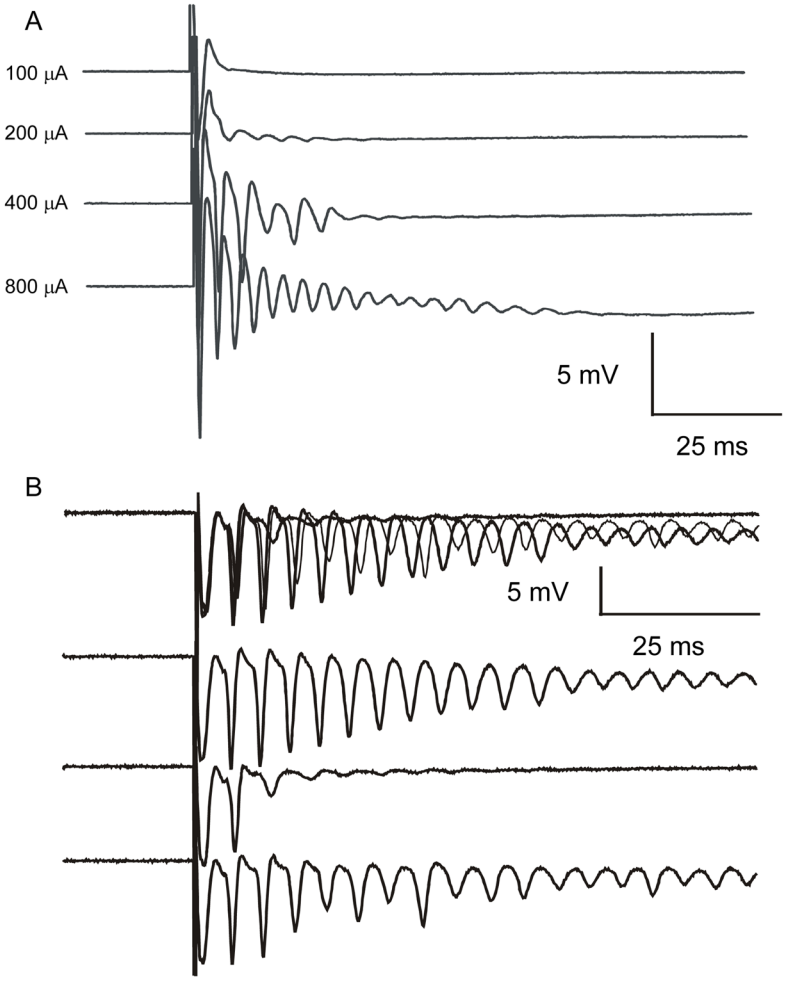

Figure 6.

Burst discharges recorded from the granule cell layer after hilar stimulation in slices from the ipsilateral hippocampus of a rat from the sham-surgery control group (A) and a rat from the experimental group several months after H-I treatment (B). All recordings were made in 6 mM $[K^+]_o$ and 30 μM bicuculline with antidromic stimulation. Panel A illustrates a graded response to hilar stimulation in a slice from a sham control rat. The number of population spikes progressively increased as the stimulus intensity increased from 100 μA to 800 μA. In the ipsilateral hippocampal slices recorded from rats several months after H-I treatment, graded increases in stimulus intensity yielded all-or-none bursts (not graded bursts). Panel B shows superimposed responses to three stimuli at 400 μA and 0.2 Hz. The three lower traces are the individual responses shown in the upper trace. In the middle individual trace, note the failure of the slice to generate a long burst of population spikes. Prolonged bursts were seen prior to (upper individual trace) and following (lower individual trace) the burst failure.

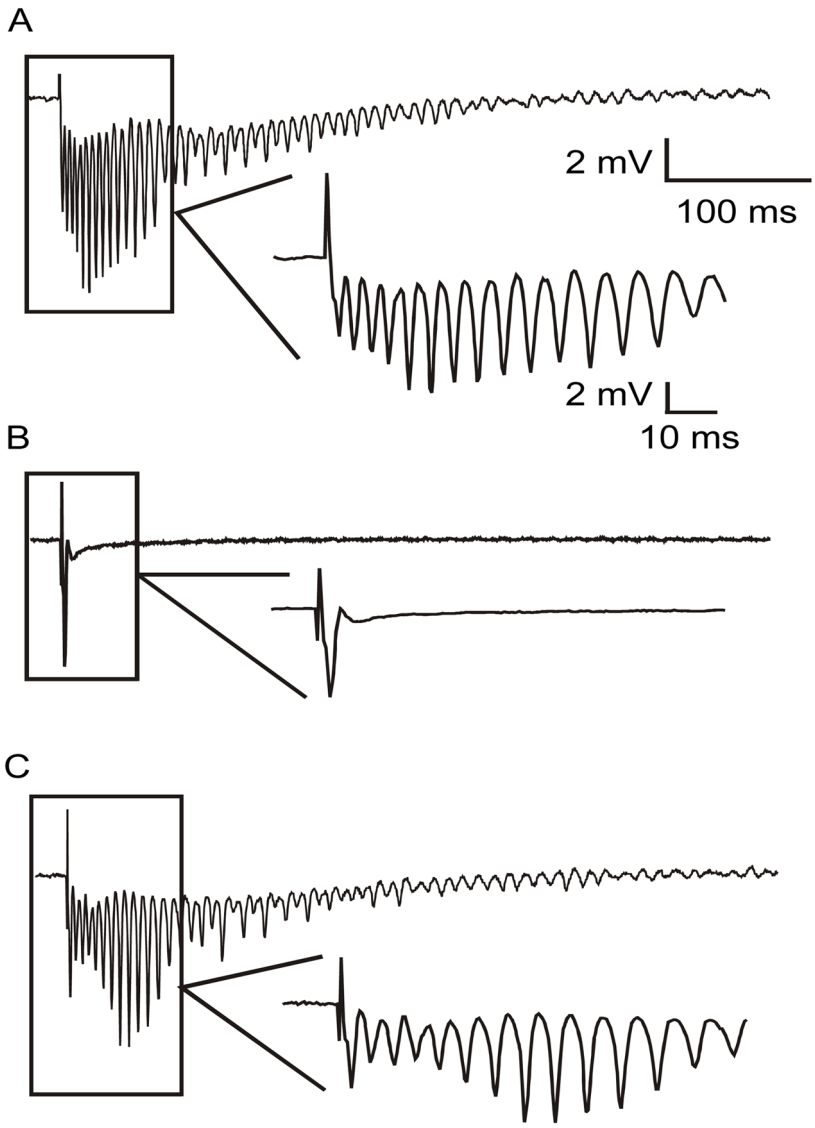

Figure 7.

Pharmacological evidence that glutamatergic synapses mediated the all-or-none network bursts recorded from the ipsilateral hippocampi of the H-I rats. Panel A shows a burst of population spikes to hilar stimulation in 6 mM $[K^+]_o$ and 30 μM bicuculline. Panel B shows recordings from the same slice while bathed in the same solution above, with the addition of 50 μM AP-5 and 50 μM DNQX. Note the complete blockade of the burst of population spikes from panel A. Panel C shows the response from the same slice after 120 min of washout of the AP-5 and DNQX (i.e., back to 6 mM $[K^+]_o$ and 30 μM bicuculline. The all-or-none burst returned with the washout of the glutamate antagonists.

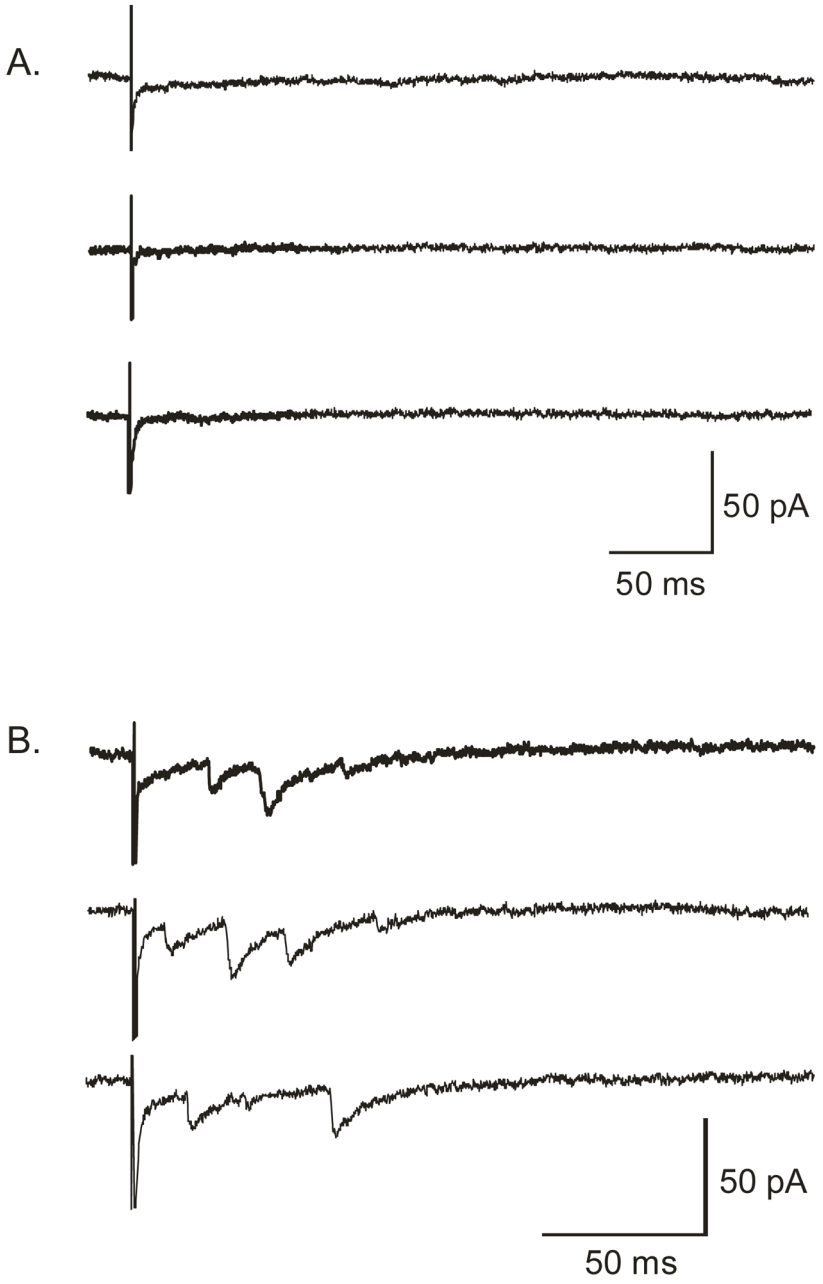

Figure 8.

Focal flash photolysis of caged glutamate was applied to the granule cell layer to test for local excitatory circuits in the dentate gyrus. Whole cell responses were recorded from granule cells; responses are shown to photostimulation in the nearby granule cell layer from a sham-surgical control rat (A) and from an H-I-treated rat (B). Both panels show whole-cell patch-clamp recordings at resting membrane potential (H-I-treated animal = −77 mV; control rat = −75 mV, corrected for the liquid junction potential). The granule cell from the HI-treated animal was located in the middle of the outer blade, and photostimulation was applied at the end of the outer blade at a distance of approximately 150 μm. The granule cell from the sham-surgical control was located in the apex, and the flash was applied approximately 300 μm away in the inner blade.

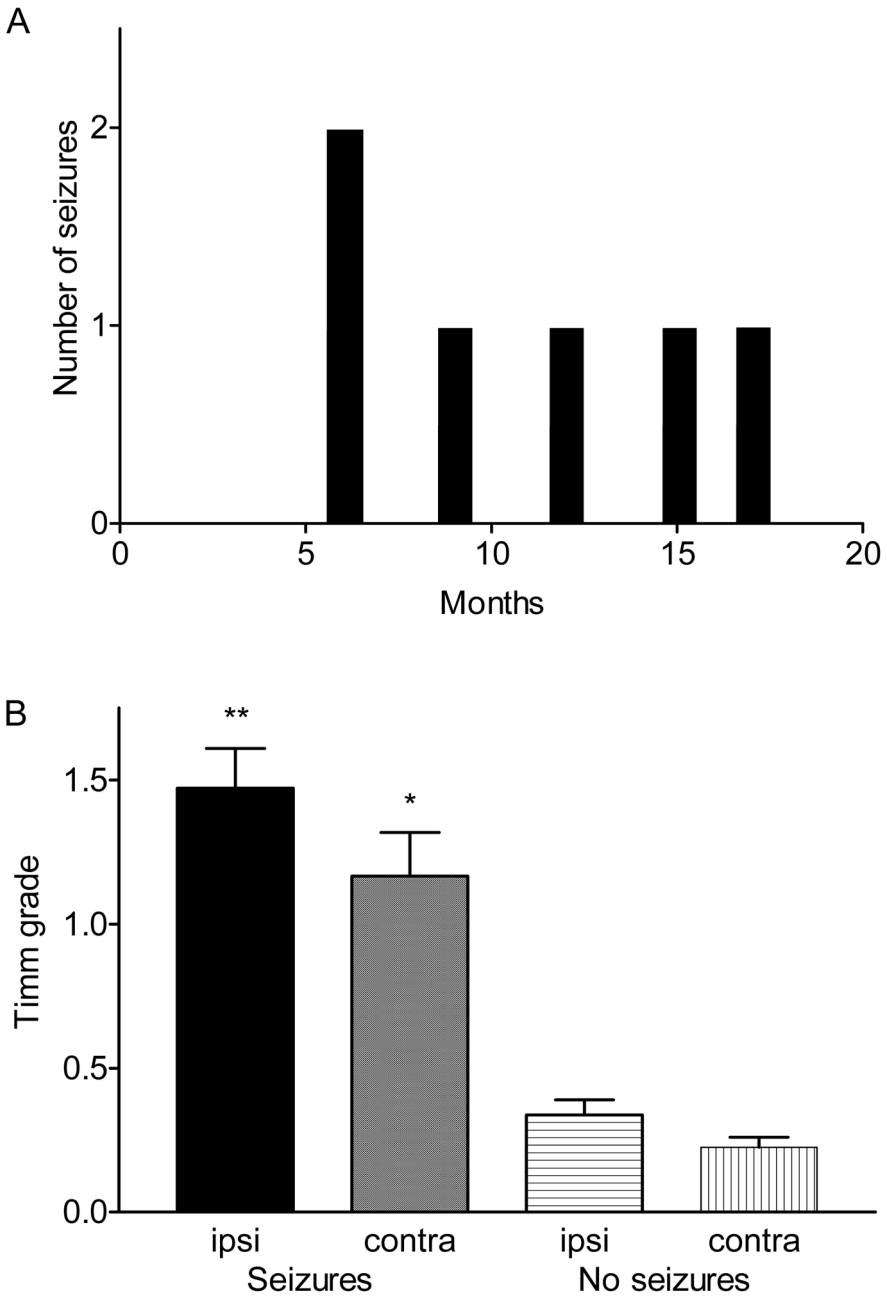

Figure 9.

Observation of motor seizures as a function of time after H-I insult and in association with the presence of Timm stain in the IML. The rats with observed seizures (n=3) survived for 18 months after H-I. Panel A shows the occurrence of seizures at different months after the H-I injury for those rats that were seen to have seizures. Panel B shows that the animals with motor seizures had significantly more Timm stain in the IML of both the ipsilateral and contralateral hippocampi compared to the lesioned rats with no seizures ($p<0.001$, Kruskal-Wallis, the median Timm stain score was 1.5, with a range of 0.5–2.0 for the ipsilateral IML in rats with seizures; the median Timm stain score was 1, with a range of 0.5–2.0 for the contralateral IML in rats with seizures; the median Timm stain score was 0, with a range of 0–1.0 for the ipsilateral

IML in rats without seizures; the median Timm stain score was 0, with a range of 0–0.5 for the contralateral IML in rats without seizures). Timm stain in the ipsilateral hippocampi from rats with seizures (double asterisk) was also significantly elevated ($p<0.05$, Kruskal-Wallis) as compared to the contralateral hippocampus from the same rats (single asterisk). Scores are shown as an average and SEM.